
Subadditivity of Probability Divergences on Bayes-Nets with Applications to Time Series GANs

Mucong Ding¹ Constantinos Daskalakis² Soheil Feizi¹

Abstract

GANs for time series data often use sliding windows or self-attention to capture underlying time dependencies. While these techniques have no clear theoretical justification, they are successful in significantly reducing the discriminator size, speeding up the training process, and improving the generation quality. In this paper, we provide both theoretical foundations and a practical framework of GANs for high-dimensional distributions with conditional independence structure captured by a Bayesian network, such as time series data. We prove that several probability divergences satisfy subadditivity properties with respect to the neighborhoods of the Bayes-net graph, providing an upper bound on the distance between two Bayes-nets by the sum of (local) distances between their marginals on every neighborhood of the graph. This leads to our proposed *Subadditive GAN* framework that uses a set of simple discriminators on the neighborhoods of the Bayes-net, rather than a giant discriminator on the entire network, providing significant statistical and computational benefits. We show that several probability distances including Jensen-Shannon, Total Variation, and Wasserstein, have subadditivity or generalized subadditivity. Moreover, we prove that Integral Probability Metrics (IPMs), which encompass commonly-used loss functions in GANs, also enjoy a notion of subadditivity under some mild conditions. Furthermore, we prove that nearly all f -divergences satisfy local subadditivity in which subadditivity holds when the distributions are relatively close. Our experiments on synthetic as well as real-world datasets verify the proposed theory and the benefits of subadditive GANs.

1. Introduction

Generative Adversarial Networks (GANs) (Goodfellow et al., 2014) have been successfully used to model complex real-world distributions such as image data. However, they face challenges in applications involving time-series data. A proper generative model for time-series data should identify the complex temporal dependencies underlying the conditional distributions $P_{X_t|X_{t-1}, \dots, X_1}$. When the X_t 's are high-dimensional, the time-horizon is large, and the GAN is not endowed with appropriate “inductive bias”—incorporating knowledge about the distribution such as (when the distribution is known to be sampled by a Markov Chain) that “ X_t is conditionally independent of X_{t-2} conditioning on X_{t-1} ”—GANs face challenges in identifying the temporal dependencies underlying the data on their own.

These challenges have naturally motivated several generator and discriminator designs based on sliding windows (Li et al., 2019), hierarchical sampling (Liu et al., 2019), self-attention (Clark et al., 2019), recurrent neural networks (Esteban et al., 2017; Mogren, 2016), dilated causal convolutions (Oord et al., 2016; Donahue et al., 2019), etc. These models have been applied to a wide range of tasks including imputation (Liu et al., 2019), anomaly detection (Li et al., 2019), and generation of time-series data (Esteban et al., 2017; Mogren, 2016), such as voice (Oord et al., 2016; Donahue et al., 2019), music (Engel et al., 2019; Dong et al., 2018) and videos (Clark et al., 2019). Intuitively, these methods aim at structuring the generation process and/or narrowing down the purview of the discriminator to capture known dependencies leading to improved computational and statistical properties. These methods, however, are mostly not accompanied with theoretical foundations.

In this work, we propose a theoretically-founded GAN framework addressing the afore-described challenges. Let P be a target distribution generating data over n time steps, sampling vector (X_1, X_2, \dots, X_n) where $X_i \in \mathbb{R}^d$. Let Q be the distribution generated by a generator network. How might we structure a discriminator network whose job is to discriminate between P and Q ? One way to do so, following the original GAN formulation (Goodfellow et al., 2014; Arjovsky et al., 2017), is to ignore any conditional independence structure we might know about P , letting the

¹Department of Computer Science, University of Maryland, College Park, Maryland, USA ²Department of Electrical Engineering and Computer Science, Massachusetts Institute of Technology, Cambridge, Massachusetts, USA. Correspondence to: Mucong Ding <mcding@cs.umd.edu>, Soheil Feizi <sfeizi@cs.umd.edu>.

GAN to “learn it on its own.” In this case, each vectorized sample from the generator or the target distribution will be viewed as a vector in \mathbb{R}^{nd} , and the discriminator network will take nd inputs. Note that the number of inputs to the discriminator increases with the number of observations in time, i.e., n . This can lead to very large discriminator networks, especially in applications where data is gathered across many time steps. In turn, large discriminators face computational and statistical challenges, given that min-max training is computationally challenging, and statistical hypothesis testing in large dimensions requires sample complexity exponential in the dimension; see e.g. discussion in (Daskalakis & Pan, 2017).

Our work tackles these challenges by considering target distributions that are high-dimensional but can be modeled as Bayesian networks with small in-degree. Markov Chains are special cases of such distributions in which every node in the network represents a time step. The pertinent question is whether a known Bayes-net structure can be exploited to design a GAN whose discriminators are simpler. In particular, we are interested in whether we can replace the large discriminator of the vanilla GAN implementation with several simple discriminators that are used to enforce constraints on local neighborhoods of the Bayes-net. We provide an affirmative answer to this question for several popular GANs based on Jensen–Shannon divergences—e.g. the original GAN of Goodfellow et al. (2014), f -divergences—e.g. f -GAN by Nowozin et al. (2016), and Integral Probability Metrics (IPMs) (Müller, 1997)—e.g. Wasserstein GAN (Arjovsky et al., 2017), MMD-GAN (Li et al., 2015) and Energy-based GAN (Zhao et al., 2017).

Our proposed framework is based on *subadditivity* properties of divergences and probability metrics over a Bayes-net, which provide an upper bound on the distance between two distributions with the same Bayes-net structure by the sum of distances between their marginals on every local neighborhood of the Bayes-net (Daskalakis & Pan, 2017). Each local neighborhood is defined as the union of a node i and its parents Π_i , as it is the smallest set that encodes conditional dependence. This leads to our proposed *Subadditive GAN* framework (Fig. 1) that uses a set of simple (local) discriminators on the neighborhoods of the Bayes-net, rather than a large discriminator on the entire network, providing significant statistical and computational benefits.

In particular, let δ be some divergence or probability metric of interest, such as some Wasserstein distance or f -divergence. Our ideal would be to train a generator that samples a distribution Q minimizing $\delta(P, Q)$, where P is the target distribution. If $\delta(\cdot, \cdot)$ satisfies subadditivity, $\delta(P, Q)$ is upper-bounded by $\sum_{i=1}^n \delta(P_{X_i \cup X_{\Pi_i}}, Q_{X_i \cup X_{\Pi_i}})$, the sum of distances/divergences between P ’s and Q ’s marginals in local neighborhoods. In this case, our proposed subadditive

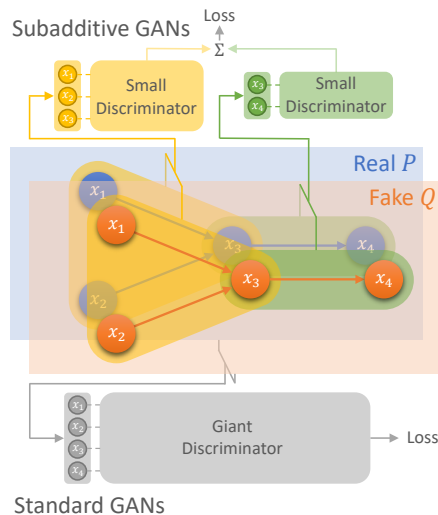


Figure 1. Comparison between our theoretical-justified subadditive GANs and the standard GANs.

GAN targets minimizing the upper bound, via local discriminators discriminating $P_{X_i \cup X_{\Pi_i}}$ against $Q_{X_i \cup X_{\Pi_i}}$, for all i . Since, in many applications, local neighborhoods can be significantly smaller than the entire graph, local discriminators targeting each of these neighborhoods will enjoy improved computational and statistical properties in comparison to a global discriminator targeting the entire graph.

The next question is which divergences or metrics exhibit subadditivity to be exploited in our proposed subadditive GAN framework. Daskalakis & Pan (2017) shows that squared Hellinger distance (H^2) and Kullback-Leibler divergence (KL) satisfy subadditivity, and they exploit it for testing the identity of Bayes-nets. They also show that Total Variation distance (TV) satisfies the subadditivity bound up to a constant factor, a property we term generalized linear subadditivity. Since our goal in this paper is to exploit subadditivity in the design of GANs, we are interested in establishing subadditivity or generalized subadditivity bounds for distances and divergences that are commonly used in GAN formulations. In Section 3, we start by showing that the Jensen-Shannon divergence (JS) used in (Goodfellow et al., 2014) satisfies generalized linear subadditivity. Next, we study the subadditivity of the Wasserstein distance used in (Arjovsky et al., 2017). We provide a counter-example for 2-Wasserstein distance W_2 , showing a pair of 3-dimensional Gaussians for which W_2 fails to satisfy subadditivity. However, using TV subadditivity, it is easy to show that all p -Wasserstein distances W_p for $p \geq 1$ satisfy linear subadditivity when the sample space is discrete and finite.

Many practical GAN frameworks such as Wasserstein GANs (Arjovsky et al., 2017), MMD-GANs (Li et al., 2015), and Energy-based GANs (Zhao et al., 2017) aim to minimize an Integral Probability Metric (IPM) (Müller, 1997)

$d_{\mathcal{F}}$ where \mathcal{F} represents the family of functions expressible in the parametric form of the discriminator. In practice, \mathcal{F} is a family of deep networks with nonlinear activation functions such as ReLUs. In Section 4, we prove that the sum of IPMs between local marginals of P and Q upper bounds the squared 1-Wasserstein distance $W_1(P, Q)$ up to some constant coefficient and additive error, i.e.

$$\alpha W_1^2(P, Q) - \epsilon \leq \sum_{i=1}^n d_{\mathcal{F}_i}(P_{X_i \cup X_{\Pi_i}}, Q_{X_i \cup X_{\Pi_i}})$$

given three conditions: (1) the sample space is bounded; (2) densities exist and $\log(P_{X_i \cup X_{\Pi_i}}/Q_{X_i \cup X_{\Pi_i}})$ is bounded and Lipschitz continuous for all i ; and (3) each local discriminator function class \mathcal{F}_i contains at least the set of single-neuron functions with bounded parameters and a ReLU activation (which is often the case in practice). Thus, IPMs can be used in a principled manner in the subadditive GAN framework. Finally, in Section 5, we study *local* subadditivity of divergences for P and Q that are close to each other (e.g., after several steps of training). In this case, we prove that all f -divergences whose $f(\cdot)$ is continuous and has a positive second-order derivative at 1 satisfy linear subadditivity.

In summary, our results show that several popular divergences and metrics can be used, in a principled way, in our proposed subadditive GAN framework (Fig. 1). Subadditive GANs not only utilize the conditional independence information in a natural way but also decompose the high-dimensional distributions into low-dimensional marginals. Since subadditive GANs have simple discriminators, they enjoy fast training as well as improved generalization. In Section 6, we show that subadditive GANs outperform the standard GAN formulations in terms of the generated sample diversity, fidelity, and usefulness, on various data-types including autoregressive time series and Bayes-nets. We also compare subadditive GANs to other popular designs of time-series GANs, including RGAN (Esteban et al., 2017) and WaveGAN (Donahue et al., 2019) on the basketball player trajectory dataset (Felsen et al., 2018). Our simple framework achieves the same level of performance compared to these methods while being rigorously founded.

In summary, we make the following contributions:

- We introduce subadditive GANs, a theoretically-founded GAN framework for modeling high-dimensional distributions with Bayes-net structure.
- We prove that several popular divergences and probability metrics used in practical GANs satisfy different notions of subadditivity. Thus, their use in subadditive GANs is theoretically justified. These measures include Jensen-Shannon divergence and other f -divergences, Wasserstein distances, IPMs, etc.
- Over several synthetic and real datasets, we show the effectiveness of subadditive GANs in terms of training stability and generation quality.

2. Problem Setup and Prior Work

2.1. Preliminaries and Notations

Consider a Directed Acyclic Graph (DAG) G . Let Π_i be the set of parents of node $i \in \{1, \dots, n\}$ in G . Assume that $(1, \dots, n)$ is a topological ordering of G , i.e. $\Pi_i \subseteq \{1, \dots, i-1\}$ for all i . A probability distribution $P(x)$ defined over space $\Omega = \{(x_1, \dots, x_n)\}$ is a *Bayes-net with respect to graph G* if it can be factorized as $P(x) = \prod_{i=1}^n P_{X_i|X_{\Pi_i}}(x_i|x_{\Pi_i})$.

For two probability distributions P and Q on the same sample space Ω , the f -divergence of P from Q , denoted $D_f(P, Q)$, is defined as,

$$D_f(P, Q) := \int_{\Omega} f\left(\frac{dP}{dQ}\right) dQ$$

If densities exist, $D_f(P, Q) = \int_{\Omega} f\left(\frac{P(x)}{Q(x)}\right) Q(x)dx$. In this definition, the function $f: \mathbb{R}_+ \rightarrow \mathbb{R}$ is a convex, lower-semi-continuous function satisfying $f(1) = 0$. We can define $f(0) = \lim_{t \downarrow 0} f(t) \in \mathbb{R} \cup \{\infty\}$. Every convex, lower semi-continuous function f has a convex conjugate function f^* , defined as $f^* = \sup_{u \in \text{dom}_f} \{ut - f(u)\}$. Common f -divergences are Total Variation distance (TV), squared Hellinger distance (H^2), Kullback-Leibler divergence (KL), Jeffrey divergence (JF), and Jensen-Shannon divergence (JS); see Appendix B.

Suppose Ω is a metric space with distance $d(\cdot, \cdot)$. The p -Wasserstein distance W_p is defined as,

$$W_p(P, Q) := \left(\inf_{\gamma \in \Gamma(P, Q)} \int_{\Omega \times \Omega} d(x, y)^p d\gamma(x, y) \right)^{\frac{1}{p}}$$

where $\gamma \in \Gamma(P, Q)$ denotes the set of all possible couplings of P and Q ; see Appendix C for details.

In this paper, unless otherwise noted, we always assume $X_i \in \mathbb{R}^d$, $\Omega \subseteq \mathbb{R}^{nd}$, and use the Euclidean metric. We always assume the density exists. Furthermore, for discussions on f -divergences, we always assume P is absolutely continuous with respect to Q , written as $P \ll Q$.

2.2. Subadditivity and Markov Property

In this section, we review the notion of *subadditivity of a statistical divergence δ on Bayes-nets*.

Definition 1 (Subadditivity of Divergence on Bayes-nets). *Consider two Bayes-nets P, Q over the same sample space $\Omega = \{(x_1, \dots, x_n)\}$ and defined with respect to the same DAG, G , i.e. factorizable as follows:*

$$\begin{aligned} P(x) &= \prod_{i=1}^n P_{X_i|X_{\Pi_i}}(x_i|x_{\Pi_i}) \\ Q(x) &= \prod_{i=1}^n Q_{X_i|X_{\Pi_i}}(x_i|x_{\Pi_i}) \end{aligned} \quad (1)$$

where Π_i is the set of parents of i in G . If a statistical divergence δ satisfies

$$\delta(P, Q) \leq \sum_{i=1}^n \delta(P_{X_i \cup X_{\Pi_i}}, Q_{X_i \cup X_{\Pi_i}}) \quad (2)$$

for every P and Q as above, we say that δ satisfies subadditivity on Bayes-nets. More generally, if δ satisfies

$$\alpha \cdot \delta(P, Q) \leq \sum_{i=1}^n \delta(P_{X_i \cup X_{\Pi_i}}, Q_{X_i \cup X_{\Pi_i}}), \quad (3)$$

for some constant $\alpha > 0$, we say that δ satisfies α -linear subadditivity on Bayes-nets.

We refer to the right hand side of Eq. (2) and Eq. (3), $\sum_{i=1}^n \delta(P_{X_i \cup X_{\Pi_i}}, Q_{X_i \cup X_{\Pi_i}})$, as the subadditivity upper bound, and to $\Delta = \sum_{i=1}^n \delta(P_{X_i \cup X_{\Pi_i}}, Q_{X_i \cup X_{\Pi_i}}) - \delta(P, Q)$ as the subadditivity gap. If a statistical divergence δ satisfies subadditivity or linear subadditivity, minimizing the subadditivity upper bound leads to the minimization of $\delta(P, Q)$. The subadditivity upper bound is used as the objective function in the proposed subadditive GANs.

We argue that subadditivity of $\delta(P, Q)$ with respect to (1) product measures, and (2) length 3 Markov Chains, suffices to imply subadditivity on all Bayes-nets. The claim is implicit in the proof of Theorem 2.1 of (Daskalakis & Pan, 2017); we state it explicitly here and provide its proof in Appendix A.1 for completeness. Roughly speaking, the proof follows because we can always combine nodes of a Bayes-net into super-nodes to obtain a 3-node Markov Chain or a 2-node product measure, and apply the Markov Chain/Product Measure subadditivity property recursively.

Theorem 1. *If a divergence δ satisfies the following:*

(1) *For any two Bayes-nets P and Q on DAG $X \rightarrow Y \rightarrow Z$, the following subadditivity holds:*

$$\delta(P_{XYZ}, Q_{XYZ}) \leq \delta(P_{XY}, Q_{XY}) + \delta(P_{YZ}, Q_{YZ})$$

(2) *For any two product measures P and Q over variables X and Y , the following subadditivity holds:*

$$\delta(P_{XY}, Q_{XY}) \leq \delta(P_X, Q_X) + \delta(P_Y, Q_Y)$$

then δ satisfies subadditivity on Bayes-nets.

Using Theorem 1, it not hard to show that squared Hellinger distance (H^2) is subadditive on Bayes-nets, as proven by Daskalakis & Pan (2017). For completeness, we provide proof of the following in Appendix A.2.

Theorem 2 (Theorem 2.1 of Daskalakis & Pan (2017)). *The squared Hellinger distance*

$$H^2(P, Q) := \frac{1}{2} \int (\sqrt{P} - \sqrt{Q})^2 dx = 1 - \int \sqrt{PQ} dx$$

has subadditivity on Bayes-nets.

The subadditivity theorem of H^2 give us a simple condition for equality of two Bayes-nets: $\forall i, P_{X_i \cup X_{\Pi_i}} = Q_{X_i \cup X_{\Pi_i}}$.

3. Subadditivity of Statistical Divergences

In this section, we first prove the subadditivity of KL-divergence (KL) and Jeffrey divergence (JF). We disprove the subadditivity of 2-Wasserstein distance (W_2) by a counter-example comprising two 3-dimensional Gaussians.

We then prove the linear subadditivity of Jensen-Shannon divergence (JS) and the Total Variation distance (TV). Moreover, based on TV's result, we prove that all p -Wasserstein distances (W_p) with $p \geq 1$ satisfy linear subadditivity when space Ω is finite. Numerical verification of the subadditivity can be found in Appendix J.

3.1. Subadditivity of KL and Jeffrey Divergences

The subadditivity of KL-divergence (KL) on Bayes-nets is claimed in (Daskalakis & Pan, 2017) without a proof. We provide a proof in Appendix A.3 for completeness.

Theorem 3 (Claimed in (Daskalakis & Pan, 2017)). *The KL-divergence defined as*

$$\text{KL}(P, Q) := \int P \log \left(\frac{P}{Q} \right) dx$$

has subadditivity on Bayes-nets.

It follows from the proof of Theorem 3 that the following conditions suffice for the KL subadditivity to become additivity: $\forall i, P_{X_{\Pi_i}} = Q_{X_{\Pi_i}}$ (almost everywhere). From the investigation of local subadditivity of f -divergences (Theorem 9 in Section 5), we will see that this is the minimum set of requirements possible. We conclude by noting that the subadditivity of KL divergence easily implies the subadditivity of the Jeffrey divergence.

Corollary 4. *The Jeffrey divergence defined as*

$$\text{JF}(P, Q) := \text{KL}(P, Q) + \text{KL}(Q, P)$$

has subadditivity on Bayes-nets.

3.2. Counter-Examples for the 2-Wasserstein Distance

In this section, we list a counter-example of the subadditivity of the Wasserstein distance W_2 using Gaussian distributions in \mathbb{R}^3 . We state our construction and verify that the distributions P, Q share the same probabilistic structure. Then, a numerical plot (Fig. 2) shows that the desired inequality is violated. That is, W_2 does not have the subadditivity property.

Consider the Markov Chain $X \rightarrow Y \rightarrow Z$ for a non-degenerate Gaussian $(X, Y, Z) \sim \mathcal{N}(m, C)$ on \mathbb{R}^3 (Markov Random Field is the most appropriate probability graphical model to describe such Gaussian, but it is also a valid Bayes-net; see Appendix E.1). It can be verified that the Markov property $P(Z|X, Y) = P(Z|Y)$ holds if and only if the

2×2 upper-right (or equivalently, the lower-left) sub-matrix of the covariance matrix C has zero determinant, which can be written as $\text{Var}[Y]\text{Cov}[X, Z] = \text{Cov}[X, Y]\text{Cov}[Y, Z]$.

Counter-Example 1. Consider two 3-dimensional Gaussians $P^x = \mathcal{N}(\mathbf{0}, C_1)$, $Q^{xy} = \mathcal{N}(\mathbf{0}, C_2)$, where,

$$C_1 = \begin{bmatrix} 1 & x & 0 \\ x & 1 & 0 \\ 0 & 0 & 1 \end{bmatrix} \quad C_2 = \begin{bmatrix} 1 & x & xy \\ x & 1 & y \\ xy & y & 1 \end{bmatrix}$$

and $\mathbf{0} \in \mathbb{R}^3$ is the zero vector. The two distributions have a Markov Chain structure $X \rightarrow Y \rightarrow Z$, since the 2×2 upper-right (or lower-left) sub-matrix of C_1 and C_2 has zero determinant. The distance $W_2(P^x, Q^{xy})$ depends on parameters (x, y) . For all $(x, y) \in \{(x, y) \in \mathbb{R}^2 | 0 < x, y < 1\}$, we have $W_2(P_{XYZ}^x, Q_{XYZ}^{xy}) > W_2(P_{XY}^x, Q_{XY}^{xy}) + W_2(P_{YZ}^x, Q_{YZ}^{xy})$, which violates the subadditivity inequality of W_2 .

Counter-Example 1 can be verified numerically, as the W_2 distance between Gaussians can be exactly computed using the formula in Theorem 20 in Appendix C.1. As shown in Fig. 2, the subadditivity gap Δ is negative, thus the subadditivity bound is violated.

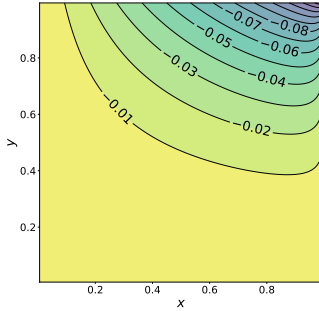


Figure 2. Contour maps showing the counter-example of subadditivity of 2-Wasserstein distance W_2 . The two distributions P^x, Q^{xy} are 3-dimensional Gaussians $P^x = \mathcal{N}(\mathbf{0}, C_1)$, $Q^{xy} = \mathcal{N}(\mathbf{0}, C_2)$ with Markov Chain structure $X \rightarrow Y \rightarrow Z$. The contours and colors indicate the subadditivity gap $\Delta = W_2(P_{XY}^x, Q_{XY}^{xy}) + W_2(P_{YZ}^x, Q_{YZ}^{xy}) - W_2(P_{XYZ}^x, Q_{XYZ}^{xy})$.

This straightforward but fundamental counter-example shows that Wasserstein’s subadditivity does not hold even if all distributions are Gaussians. For many common divergences including Jensen-Shannon divergence (JS) and p -Wasserstein distance (W_p), we should seek the generalized form of subadditivity: linear subadditivity.

3.3. Generalized Linear Subadditivity

The linear subadditivity of Jensen-Shannon divergence (JS) follows from the subadditivity property of squared Hellinger distance (H^2); see Appendix A.4.

Corollary 5. Jensen-Shannon divergence

$$\text{JS}(P, Q) := \frac{1}{2} \text{KL} \left(P, \frac{P+Q}{2} \right) + \frac{1}{2} \text{KL} \left(Q, \frac{P+Q}{2} \right)$$

satisfies ln 2-linear subadditivity on Bayes-nets.

Using a slightly modified version of Theorem 1, it is not hard to derive the linear subadditivity of Total Variation distance (TV), which is stated without proof in (Daskalakis & Pan, 2017). We provide a proof in Appendix A.5 for completeness.

Theorem 6 (Claimed in Daskalakis & Pan (2017)). The Total Variation distance

$$\text{TV}(P, Q) := \frac{1}{2} \int |P - Q| dx$$

satisfies $\frac{1}{2}$ -linear subadditivity on Bayes-nets.

Whenever Ω is a finite (and therefore bounded) metric space, there exist two-way bounds between p -Wasserstein distance and Total Variation distance, namely $W_p(P, Q)^p / \text{diam}(\Omega)^p \leq \text{TV}(P, Q) \leq W_p(P, Q)^p / d_{\min}^p$, where $\text{diam}(\Omega) = \max\{d(x, y) | x, y \in \Omega\}$ is the diameter of Ω and $d_{\min} = \min_{x \neq y} d(x, y)$ is the smallest distance in Ω (Theorem 21 in Appendix C.1). This directly implies the linear subadditivity of p -Wasserstein distance on finite Ω , via Theorem 6.

Corollary 7. If Ω is a finite metric space, p -Wasserstein distance for $p \geq 1$ satisfies $(d_{\min}/2^{1/p} \text{diam}(\Omega))$ -linear subadditivity on Bayes-nets, where $\text{diam}(\Omega)$ is the diameter and d_{\min} is the smallest distance between pairs of distinct points in Ω .

4. Subadditivity of IPMs

In this section, we study subadditivity of Integral Probability Metrics (IPMs) (Müller, 1997), which are used in popular GAN formulations such as Wasserstein GANs (Arjovsky et al., 2017), MMD-GANs (Li et al., 2015) and Energy-based GANs (Zhao et al., 2017), defined as

$$d_{\mathcal{F}}(P, Q) := \sup_{\phi \in \mathcal{F}} \{ \mathbb{E}_{x \sim P}[\phi(x)] - \mathbb{E}_{x \sim Q}[\phi(x)] \}$$

The IPM with \mathcal{F} being all 1-Lipschitz functions is equivalent to 1-Wasserstein distance W_1 (Villani, 2008). Practical GANs take \mathcal{F} as a parametric function class, $\mathcal{F} = \{\phi_{\theta}(x) | \theta \in \Theta\}$, where $\phi_{\theta}(x)$ is a neural network.

We upper bound the squared 1-Wasserstein distance $W_1^2(P, Q)$ by the sum of IPMs on the local marginals, $\sum_{i=1}^n d_{\mathcal{F}_i}(P_{X_i \cup X_{\Pi_i}}, Q_{X_i \cup X_{\Pi_i}})$ (we call it the IPM subadditivity upper-bound) up to some constant coefficient and additive error. Such property will provide a theoretical justification for subadditive GANs based on IPMs. That is, their objective minimizes an upper bound on the 1-Wasserstein distance.

Theorem 8. Consider distributions P, Q on $\Omega = \{(X_1, \dots, X_n)\} \subseteq \mathbb{R}^{nd}$ with a common Bayes-net structure G , and any set of function classes $\{\mathcal{F}_1, \dots, \mathcal{F}_n\}$, satisfying the following three conditions:

- (1) The space Ω is bounded, i.e. $\text{diam}(\Omega) < \infty$.
- (2) Each discriminator class \mathcal{F}_i is larger than the set of single neuron networks with ReLU activations, i.e. $\forall i, \mathcal{F}_i \supseteq \{\max\{w^T x + b, 0\} \mid \| [w, b] \|_2 = 1\}$.
- (3) $\log(P_{X_i \cup X_{\Pi_i}}/Q_{X_i \cup X_{\Pi_i}})$ are bounded and Lipschitz continuous for all i .

Then, we have the subadditivity upper bound of IPMs on the squared 1-Wasserstein distance between P and Q , i.e.,

$$\alpha W_1^2(P, Q) - \epsilon \leq \sum_{i=1}^n d_{\mathcal{F}_i}(P_{X_i \cup X_{\Pi_i}}, Q_{X_i \cup X_{\Pi_i}})$$

where $\alpha, \epsilon > 0$ are constants independent of P, Q and \mathcal{F} .

Regarding condition (1), bounded space Ω still allows many real-world data-types, including images and videos. Regarding condition (2), all practical neural networks using ReLU activations satisfy this requirement. Thus, the only non-trivial requirement is the condition (3). In practical GAN training, Q is the output distribution of a generative model, which can be regarded as a transformation of a Gaussian distribution. Thus, in general, Q is bounded and Lipschitz. If we have $P \ll Q$, for bounded and Lipschitz real distribution P , the condition (3) is satisfied.

Proof of Theorem 8 is based on the subadditivity property of Jeffrey divergence (JF) (Corollary 4). Firstly, it makes use of Proposition 2.7 and Corollary 2.9 in (Zhang et al., 2018) (repeated as Theorem 23 in Appendix F.3) to upper bound $\text{JF}(P_{X_i \cup X_{\Pi_i}}, Q_{X_i \cup X_{\Pi_i}})$ by a function of $d_{\mathcal{F}_i}(P_{X_i \cup X_{\Pi_i}}, Q_{X_i \cup X_{\Pi_i}})$, given that $\log(P_{X_i \cup X_{\Pi_i}}/Q_{X_i \cup X_{\Pi_i}})$ is in the closure of the linear span of \mathcal{F}_i . This is not a hard requirement. From Corollary 2.4 in (Zhang et al., 2018), we know as long as $\mathcal{F}_i \supseteq \{\max\{w^T x + b, 0\} \mid \| [w, b] \|_2 = 1\}$, the linear span of \mathcal{F}_i is dense in the Banach space of bounded continuous functions. Moreover, since Lipschitz continuity implies ordinary continuity, conditions (2) and (3) imply the required condition above.

Secondly, we use Proposition 6 of (Bach, 2017) (repeated as Theorem 24 in Appendix F.3) to control the coefficients in such upper bound, so that $d_{\mathcal{F}_i}(P_{X_i \cup X_{\Pi_i}}, Q_{X_i \cup X_{\Pi_i}})$ can upper bound $\text{JF}(P_{X_i \cup X_{\Pi_i}}, Q_{X_i \cup X_{\Pi_i}})$ up to some bounded coefficient and additive error independent of P, Q and \mathcal{F} . Proposition 6 of (Bach, 2017) provides an efficient upper bound on the infimum of the L_∞ norm between $\log(P_{X_i \cup X_{\Pi_i}}/Q_{X_i \cup X_{\Pi_i}})$ and any function in the linear span of \mathcal{F}_i , given conditions (1), (2) and (3). Summing up the inequalities for $i = 1, \dots, n$ and using the subadditivity inequality of JF, we upper bound $\text{JF}(P, Q)$ up to some constant coefficient and additive error. In addition to this, we also use the inequality $W_1(P, Q) \leq \text{diam}(\Omega)\text{TV}(P, Q)$ for bounded Ω (a special case of Theorem 21 in Appendix C.2), and the Pinsker's inequality $\text{TV}(P, Q) \leq$

$\sqrt{\frac{1}{2}\text{KL}(P, Q)}$ (repeated as Theorem 18 in Appendix B.2), to finally upper bound the squared 1-Wasserstein distance $W_1^2(P, Q)$. For the detailed proof, see Appendix A.6.

5. Local Subadditivity

In this section, we consider the case when two distributions P, Q are close to each other. This can happen after some training steps in a GAN. We consider several notions of ‘‘closeness’’ for distributions. We show that almost all f -divergences satisfy subadditivity inequality if P, Q are ϵ -close to each other with $0 < \epsilon \ll 1$.

First, we define two notions of the closeness of distributions as follows:

Definition 2 (One- and Two-Sided ϵ -Close Distributions). *Distributions P, Q are one-sided ϵ -close for some $0 < \epsilon < 1$, if $\forall x \in \Omega \subseteq \mathbb{R}^{nd}$, $P(x)/Q(x) < 1 + \epsilon$. Moreover, P, Q are two-sided ϵ -close, if $\forall x, 1 - \epsilon < P(x)/Q(x) < 1 + \epsilon$. Note this requires $P \ll\ll Q$.*

In practical GAN training, P is the empirical distribution of observed data, and Q is the continuous distribution of generated samples (since it is a function of a Gaussian). $P \gg Q$ does not hold, and one-sided close is a better characterization of the real-world situation. Nevertheless, we study both closeness notions for completeness.

5.1. Local Subadditivity under Perturbation

In this section, for the sake of theoretical simplicity, we consider the limit $\epsilon \rightarrow 0$ for two-sided ϵ -close distributions (in Section 5.2, we will relax this assumption). We call Q a perturbation of P (Makur, 2015).

Theorem 9. *For two-sided ϵ -close distributions P, Q with $\epsilon \rightarrow 0$ on a common Bayes-net G , any f -divergence $D_f(P, Q)$ such that $f''(1) > 0$ has subadditivity up to $\mathcal{O}(\epsilon^3)$. That is,*

$$D_f(P, Q) \leq \sum_{i=1}^n D_f(P_{X_i \cup X_{\Pi_i}}, Q_{X_i \cup X_{\Pi_i}}) + \mathcal{O}(\epsilon^3)$$

Moreover, the subadditivity gap is proportional to the sum of χ^2 divergences between marginals on the set of parents of each node, up to $\mathcal{O}(\epsilon^3)$. That is,

$$\begin{aligned} \Delta &= \sum_{i=1}^n D_f(P_{X_i \cup X_{\Pi_i}}, Q_{X_i \cup X_{\Pi_i}}) - D_f(P, Q) \\ &= \frac{f''(1)}{2} \sum_{i=1}^n \chi^2(P_{\Pi_i}, Q_{\Pi_i}) + \mathcal{O}(\epsilon^3) \end{aligned}$$

Theorem 9 indicates that when P, Q are very close, the focus of the set of local discriminators falls on the differences between the marginals on the set of parents. We make use of the Taylor expansion of $f(\cdot)$ in the proof; see Appendix A.7.

	Single-Variate Time Series ($T = 10$)		Multi-Variate Time Series ($T = 5, d = 5, p = 2$)		Bayes-Nets ($n = 8$)
Settings	$p = 2$	$p = 4$	$q = 3$	$q = 5$	Fixed G
Energy Statistics (smaller is better)					
Subadditive GAN	.084±.010	.089±.009	.088±.014	.130±.016	.088±.009
Standard GAN	.323±.059	.356±.030	.236±.020	.219±.025	.206±.026
Discriminative Scores (smaller is better)					
Subadditive GAN	.716±.020	.727±.016	.803±.027	.844±.018	.810±.029
Standard GAN	.755±.014	.747±.011	.859±.012	.855±.013	.851±.019
Predictive Scores (smaller is better)					
Subadditive GAN	.052±.002	.114±.003	.023±.002	.022±.002	n/a
Standard GAN	.071±.004	.131±.006	.036±.002	.024±.002	n/a

Table 1. Results on synthetic autoregressive time series and Bayes-nets.

5.2. Linear Subadditivity for Close Distributions

In this section, we consider distributions that are one or two-sided ϵ -close with a non-infinitesimal $\epsilon > 0$. This is a more realistic setup compared to the setup of Section 5.1. The Taylor expansion approach used there is no longer applicable. However, using the methodology to prove general f -divergence inequalities (Lemma 16), and a technique of equivalent f -divergences, we are able to obtain linear subadditivity for both cases, under very mild conditions. See Appendix A.8 for the proofs.

Theorem 10. *An f -divergence whose $f(\cdot)$ is continuous on $(0, \infty)$ and twice differentiable at 1 with $f''(1) > 0$, satisfies α -linear subadditivity, when P, Q are two-sided $\epsilon(\alpha)$ -close with $\epsilon > 0$, where $\epsilon(\alpha)$ is a non-increasing function and $\lim_{\epsilon \downarrow 0} \alpha = 1$.*

Theorem 10 applies to all practical f -divergences, including KL, reverse KL, χ^2 , reverse χ^2 , and squared Hellinger H^2 divergences.

In addition to the requirements of Theorem 10, if $f(\cdot)$ is also strictly convex and $f(0) = \lim_{t \downarrow 0} f(t)$ is finite, $\forall t \in [0, 1)$, we have the following subadditivity result for one-sided close distributions.

Theorem 11. *An f -divergence whose $f(\cdot)$ is continuous and strictly convex on $(0, \infty)$, twice differentiable at $t = 1$, and has finite $f(0) = \lim_{t \downarrow 0} f(t)$, has linear subadditivity with coefficient $\alpha > 0$, when P, Q are one-sided $\epsilon(\alpha)$ -close with $\epsilon > 0$, where $\epsilon(\alpha)$ is a non-increasing function and $\lim_{\epsilon \downarrow 0} \alpha > 0$.*

Using Theorem 11, we can relax the condition $P \gg Q$, as long as $f(0) < \infty$ and $f(\cdot)$ is strictly convex. A broad class of f -divergences satisfy this; see Appendix G.

6. Experiments

In this section, we compare the performance of our proposed subadditive GANs to standard GANs on synthetic

and real datasets. We observe that subadditive GANs not only require fewer parameters and converge faster compared to standard GANs, but also outperform standard GANs in terms of the diversity, fidelity, and usefulness of generated samples. We also find that weight-sharing between the set of local discriminators can further reduce the model size, with slight or no decrease in the performance. Finally, we compare subadditive GANs to RGAN (Esteban et al., 2017), and WaveGAN (Donahue et al., 2019) on the basketball player trajectory dataset (Felsen et al., 2018), and show that subadditive GAN achieves the same level of performance compared to the baselines while being theoretically founded.

6.1. Methodology

We evaluate different generative models with a focus on two aspects: convergence rate and generated sample quality. For the comparison of convergence rates and training stability, we plot the average loss curves. For the comparison of generation quality, we consider three metrics as in (Yoon et al., 2019): (1) Diversity: We calculate energy statistics (Székely & Rizzo, 2013) between the real and fake samples, as a numerical score for how closely the fake distribution resembles the real one. (We also apply t-SNE (Maaten & Hinton, 2008) to visualize the real and fake distributions in Appendix H.) (2) Fidelity: We train a post-hoc recurrent neural network (RNN) classifier to distinguish between real and fake samples, and report the AUC scores. (3) Usefulness: We train a post-hoc RNN future predictor on fake sequences, and report the mean squared errors (MSEs) on real sequences. (This metric only applies to time-series data.) Since our advances are on the design of discriminators, in comparisons on a specific dataset, we always use the same generator and training parameters. All the results reported are averaged on five repeats. Appendix I contains additional information on synthetic datasets, model architectures, training hyper-parameters, and evaluation setups.

Subadditivity of Probability Divergences on Bayes-Nets

	Energy Statistics	Discriminative Scores	Predictive Scores
Distinct Discriminators	.052±.003	.618±.005	.036±.001
Identical Discriminators	.081±.012	.675±.015	.032±.001
Partially Weight-Sharing Discriminators	.050±.004	.634±.027	.038±.002

Table 2. Comparison between three weight-sharing schemes on synthetic single-variate time series ($T = 10, p = 2$).

	Energy Statistics	Discriminative Scores	Predictive Scores ($\times 100$)
Subadditive GAN	.031±.009	.784±.032	.044±.006
RGAN	.047±.011	.811±.026	.059±.008
WaveGAN	.029±.014	.779±.021	.067±.009

Table 3. Results on the basketball player trajectory dataset.

6.2. Experiments on Synthetic Data

Our subadditive GAN formulation is superior to the standard formulation in terms of the stability and the speed of training, as well as the quality of generated samples. To highlight these aspects, we conduct experiments on synthetic autoregressive sequences and Bayes-nets. They are defined as: (1) single-variate time series of length T , where the feature at each time conditionally depends on the features at p previous time steps, (2) multi-variate time series of length T with d distinct features per time unit, where each feature conditionally depends on the q nearby features at p previous time steps, and (3) Bayes-nets with eight nodes, with the underlying graph G being the Hasse diagram of all the 8 subsets of a 3-element set. See Appendix I for details on the synthetic datasets.

As shown in Table 1, for various settings of the synthetic data, subadditive GANs with Jensen-Shannon divergence consistently outperform standard vanilla GANs (Goodfellow et al., 2014) in terms of different quality metrics. The performance gap is larger when the length of the correlation in the temporal dimension (p) or in the feature dimension (q) is smaller. This is because, in such cases, local neighborhoods are small, and our local discriminators can better capture conditional independencies. Under such conditions, the number of parameters of a subadditive discriminator is significantly smaller than the standard one. Thus the improvement in the convergence rate is significant. This can be verified by the loss curves of subadditive and standard Wasserstein GANs (Fig. 3). See Appendix H for more experimental results.

One can reduce the number of parameters of a subadditive GAN by weight-sharing among local discriminators. This can be useful for time-series data where local temporal dependencies at different times are similar (e.g., object trajectories following invariant physical laws). We compare three schemes: distinct, identical, and partially weight-sharing discriminators on multi-variate autoregressive sequences in Table 2. We find weight-sharing discriminators can gen-

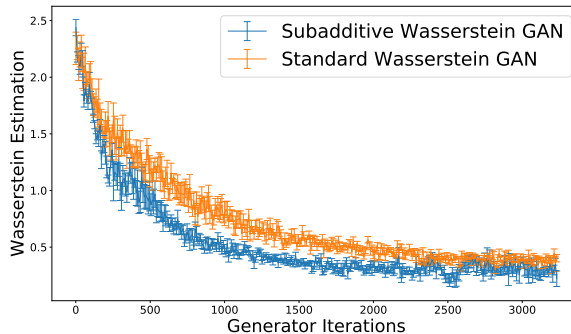


Figure 3. Estimation of Wasserstein distances at different stages of training on synthetic single-variate time series ($T = 10, p = 2$).

erate high-quality time series as the original formulation, especially in terms of sample diversity and fidelity.

6.3. Experiments on Real-World Datasets

We test subadditive GANs on the time series datasets describing movements of 5 basketball players in 12 seconds (Felsen et al., 2018) ($T = 50, d = 10$). This data contains complex temporal and spatial dynamics. The two most popular choices of GAN’s discriminator in this case are (1) recurrent neural networks (RNNs) (e.g., RGAN (Esteban et al., 2017)), and (2) dilated causal convolutions (e.g., WaveGAN (Donahue et al., 2019)). We select random subsets from the original train and test data and compare among the three models. Since the underlying conditional dependence structure is unknown, we use a grid-search to find the hypothetical temporal correlation length.

As shown in Table 3, our model achieves the same level of performance compared to the baselines in terms of energy statistics and discriminative scores, while subadditive GANs perform better than baselines in terms of the predictive score, since the focus of discriminators is more on the local dependence. See Appendix H for more experimental results.

7. Conclusions

We introduce subadditive GAN, a theoretically-founded GAN-framework for high-dimensional distributions with conditional independence captured by a Bayes-net. Sub-additive GANs use a set of simple discriminators on the neighborhoods of the Bayes-net, and provide significant statistical and computational benefits. We prove that several popular statistical divergences, IPMs, and nearly all f -divergences satisfy the general notion of subadditivity on Bayes-nets, and thus can be used in a principled way as the objective function in a subadditive GAN. Over several synthetic and real data experiments, we show the effectiveness of subadditive GANs which highlight their potentials to be used in other applications such as in generative models for video or speech.

Acknowledgements

We thank the Simons Institute for the Theory of Computing, where this collaboration started, during the “Foundations of Deep Learning” program. This project was supported in part by NSF CAREER AWARD 1942230, Simons Fellowship, Qualcomm Faculty Award, IBM Faculty Award and a sponsorship from Capital One. Constantinos Daskalakis was supported by NSF Awards IIS-1741137, CCF-1617730 and CCF-1901292, by a Simons Investigator Award, by the DOE PhILMs project (No. DE-AC05-76RL01830), by the DARPA award HR00111990021, by a Google Faculty award, and by the MIT Frank Quick Faculty Research and Innovation Fellowship.

References

- Arjovsky, M., Chintala, S., and Bottou, L. Wasserstein generative adversarial networks. In *International Conference on Machine Learning*, pp. 214–223, 2017.
- Bach, F. Breaking the curse of dimensionality with convex neural networks. *The Journal of Machine Learning Research*, 18(1):629–681, 2017.
- Clark, A., Donahue, J., and Simonyan, K. Efficient video generation on complex datasets. *arXiv preprint arXiv:1907.06571*, 2019.
- Daskalakis, C. and Pan, Q. Square hellinger subadditivity for bayesian networks and its applications to identity testing. In *Conference on Learning Theory*, pp. 697–703, 2017.
- Donahue, C., McAuley, J., and Puckette, M. Adversarial audio synthesis. In *International Conference on Learning Representations*, 2019.
- Dong, H.-W., Hsiao, W.-Y., Yang, L.-C., and Yang, Y.-H. Musegan: Multi-track sequential generative adversarial networks for symbolic music generation and accompaniment. In *Thirty-Second AAAI Conference on Artificial Intelligence*, 2018.
- Engel, J., Agrawal, K. K., Chen, S., Gulrajani, I., Donahue, C., and Roberts, A. GANSynth: Adversarial neural audio synthesis. In *International Conference on Learning Representations*, 2019.
- Esteban, C., Hyland, S. L., and Rätsch, G. Real-valued (medical) time series generation with recurrent conditional gans. *arXiv preprint arXiv:1706.02633*, 2017.
- Felsen, P., Lucey, P., and Ganguly, S. Where will they go? predicting fine-grained adversarial multi-agent motion using conditional variational autoencoders. In *Proceedings of the European Conference on Computer Vision (ECCV)*, pp. 732–747, 2018.
- Gibbs, A. L. and Su, F. E. On choosing and bounding probability metrics. *International statistical review*, 70(3):419–435, 2002.
- Goodfellow, I., Pouget-Abadie, J., Mirza, M., Xu, B., Warde-Farley, D., Ozair, S., Courville, A., and Bengio, Y. Generative adversarial nets. In *Advances in neural information processing systems*, pp. 2672–2680, 2014.
- Gulrajani, I., Ahmed, F., Arjovsky, M., Dumoulin, V., and Courville, A. C. Improved training of wasserstein gans. In *Advances in neural information processing systems*, pp. 5767–5777, 2017.
- Leshno, M., Lin, V. Y., Pinkus, A., and Schocken, S. Multilayer feedforward networks with a nonpolynomial activation function can approximate any function. *Neural networks*, 6(6):861–867, 1993.
- Li, D., Chen, D., Jin, B., Shi, L., Goh, J., and Ng, S.-K. Madgan: Multivariate anomaly detection for time series data with generative adversarial networks. In *International Conference on Artificial Neural Networks*, pp. 703–716. Springer, 2019.
- Li, Y., Swersky, K., and Zemel, R. Generative moment matching networks. In *International Conference on Machine Learning*, pp. 1718–1727, 2015.
- Liese, F. and Vajda, I. On divergences and informations in statistics and information theory. *IEEE Transactions on Information Theory*, 52(10):4394–4412, 2006.
- Liu, Y., Yu, R., Zheng, S., Zhan, E., and Yue, Y. Naomi: Non-autoregressive multiresolution sequence imputation. In *Advances in Neural Information Processing Systems*, pp. 11236–11246, 2019.

- Maaten, L. v. d. and Hinton, G. Visualizing data using t-sne. *Journal of machine learning research*, 9(Nov): 2579–2605, 2008.
- Makur, A. *A study of local approximations in information theory*. PhD thesis, Massachusetts Institute of Technology, 2015.
- Massart, P. *Concentration inequalities and model selection*, volume 6. Springer, 2007.
- Mogren, O. C-rnn-gan: Continuous recurrent neural networks with adversarial training. *arXiv preprint arXiv:1611.09904*, 2016.
- Müller, A. Integral probability metrics and their generating classes of functions. *Advances in Applied Probability*, 29(2):429–443, 1997.
- Nowozin, S., Cseke, B., and Tomioka, R. f-gan: Training generative neural samplers using variational divergence minimization. In *Advances in neural information processing systems*, pp. 271–279, 2016.
- Oberman, A. M. and Ruan, Y. An efficient linear programming method for optimal transportation. *arXiv preprint arXiv:1509.03668*, 2015.
- Olkin, I. and Pukelsheim, F. The distance between two random vectors with given dispersion matrices. *Linear Algebra and its Applications*, 48:257–263, 1982.
- Oord, A. v. d., Dieleman, S., Zen, H., Simonyan, K., Vinyals, O., Graves, A., Kalchbrenner, N., Senior, A., and Kavukcuoglu, K. Wavenet: A generative model for raw audio. *arXiv preprint arXiv:1609.03499*, 2016.
- Sason, I. and Verdu, S. f -divergence inequalities. *IEEE Transactions on Information Theory*, 62(11):5973–6006, 2016.
- Székely, G. J. and Rizzo, M. L. Energy statistics: A class of statistics based on distances. *Journal of statistical planning and inference*, 143(8):1249–1272, 2013.
- Villani, C. *Optimal transport: old and new*, volume 338. Springer Science & Business Media, 2008.
- Yoon, J., Jarrett, D., and van der Schaar, M. Time-series generative adversarial networks. In *Advances in Neural Information Processing Systems*, pp. 5509–5519, 2019.
- Zhang, P., Liu, Q., Zhou, D., Xu, T., and He, X. On the discrimination-generalization tradeoff in GANs. In *International Conference on Learning Representations*, 2018.
- Zhao, J., Mathieu, M., and LeCun, Y. Energy-based generative adversarial network. In *International Conference on Learning Representations*, 2017.

Appendix

A. Proofs

A.1. Proof of Theorem 1

Proof. The theorem is implicit in (Daskalakis & Pan, 2017). For completeness, we provide a full argument here.

For a pair of Bayes-nets P and Q with respect to a Directed Acyclic Graph (DAG) G , consider the topological ordering $(1, \dots, n)$ of the nodes of G . Consistent with the topological ordering, consider the following Markov Chain on super-nodes: $X_{\{1, \dots, n-1\} \setminus \Pi_n} \rightarrow X_{\Pi_n} \rightarrow X_n$, where Π_n is the set of parents of node n and $\Pi_n \subseteq \{1, \dots, n-1\}$. We distinguish three cases:

- $\Pi_n \neq \emptyset$ and $\Pi_n \subsetneq \{1, \dots, n-1\}$: In this case, we apply the subadditivity property of δ with respect to Markov Chains to obtain $\delta(P, Q) \leq \delta(P_{\cup_{i=1}^{n-1} X_i}, Q_{\cup_{i=1}^{n-1} X_i}) + \delta(P_{X_{\Pi_n \cup X_n}}, Q_{X_{\Pi_n \cup X_n}})$.
- $\Pi_n = \{1, \dots, n-1\}$: In this case, it is trivial that $\delta(P, Q) \equiv \delta(P_{X_{\Pi_n \cup X_n}}, Q_{X_{\Pi_n \cup X_n}}) \leq \delta(P_{\cup_{i=1}^{n-1} X_i}, Q_{\cup_{i=1}^{n-1} X_i}) + \delta(P_{X_{\Pi_n \cup X_n}}, Q_{X_{\Pi_n \cup X_n}})$.
- $\Pi_n = \emptyset$: In this case, X_n is independent from (X_1, \dots, X_{n-1}) in both Bayes-nets. Thus we apply the subadditivity of δ with respect to product measures to obtain $\delta(P, Q) \leq \delta(P_{\cup_{i=1}^{n-1} X_i}, Q_{\cup_{i=1}^{n-1} X_i}) + \delta(P_{X_n}, Q_{X_n}) \equiv \delta(P_{\cup_{i=1}^{n-1} X_i}, Q_{\cup_{i=1}^{n-1} X_i}) + \delta(P_{X_{\Pi_n \cup X_n}}, Q_{X_{\Pi_n \cup X_n}})$.

We proceed by induction. For each inductive step $k = 1, \dots, n-2$, we consider the following Markov Chain on super-nodes: $X_{\{1, \dots, n-k-1\} \setminus \Pi_{n-k}} \rightarrow X_{\Pi_{n-k}} \rightarrow X_{n-k}$. No matter what Π_{n-k} is, we always have: $\delta(P_{\cup_{i=1}^{n-k} X_i}, Q_{\cup_{i=1}^{n-k} X_i}) \leq \delta(P_{\cup_{i=1}^{n-k-1} X_i}, Q_{\cup_{i=1}^{n-k-1} X_i}) + \delta(P_{X_{\Pi_{n-k} \cup X_{n-k}}}, Q_{X_{\Pi_{n-k} \cup X_{n-k}}})$. In the end of the induction, we obtain: $\delta(P, Q) \leq \delta(P_{X_1}, Q_{X_1}) + \sum_{i=2}^n \delta(P_{\Pi_i \cup X_i}, Q_{\Pi_i \cup X_i}) \equiv \sum_{i=1}^n \delta(P_{\Pi_i \cup X_i}, Q_{\Pi_i \cup X_i})$, since $\Pi_1 \equiv \emptyset$. The subadditivity of δ on Bayes-nets is proved. \square

A.2. Proof of Theorem 2

Proof. The subadditivity of squared Hellinger distance is proved in Theorem 2.1 of (Daskalakis & Pan, 2017). Here, we repeat the proof for completeness.

Given Theorem 1, we only need to show the following:

1. For two Markov Chains P, Q on variables $X \rightarrow Y \rightarrow Z$, it holds that $H^2(P_{XYZ}, Q_{XYZ}) \leq H^2(P_{XY}, Q_{XY}) + H^2(P_{YZ}, Q_{YZ})$.
2. For two product measures P, Q on variables X, Y , it holds that $H^2(P_{XY}, Q_{XY}) \leq H^2(P_X, Q_X) + H^2(P_Y, Q_Y)$.

We first show the subadditivity with respect to Markov Chains. Using the Markov property, we know $P_{XYZ} = P_{Z|XY}P_{XY}$ (and the same holds for Q), thus,

$$\begin{aligned}
 & H^2(P_{XYZ}, Q_{XYZ}) \\
 &= 1 - \int \sqrt{P_{XYZ}Q_{XYZ}} dx dy dz \\
 &= 1 - \int \sqrt{P_{XY}Q_{XY}} \left(\int \sqrt{P_{Z|Y}Q_{Z|Y}} dz \right) dx dy \\
 &= 1 - \int \frac{1}{2}(P_Y + Q_Y) \left(\int \sqrt{P_{Z|Y}Q_{Z|Y}} dz \right) dy + \int \frac{1}{2} (\sqrt{P_{XY}} - \sqrt{Q_{XY}})^2 \left(\int \sqrt{P_{Z|Y}Q_{Z|Y}} dz \right) dx dy
 \end{aligned}$$

Since all densities are non-negative, we have $\sqrt{P_Y Q_Y} \leq \frac{1}{2}(P_Y + Q_Y)$ and $\sqrt{P_{Z|Y} Q_{Z|Y}} \leq \frac{1}{2}(P_{Z|Y} + Q_{Z|Y})$ point-

wisely. Thus,

$$\begin{aligned}
 & \mathbb{H}^2(P_{XYZ}, Q_{XYZ}) \\
 & \leq 1 - \int \sqrt{P_Y Q_Y} \left(\int \sqrt{P_{Z|Y} Q_{Z|Y}} dz \right) dy + \int \frac{1}{2} \left(\sqrt{P_{XY}} - \sqrt{Q_{XY}} \right)^2 \left(\int \frac{1}{2} (P_{Z|Y} + Q_{Z|Y}) dz \right) dx dy \\
 & = \left(1 - \int \sqrt{P_{YZ} Q_{YZ}} dy dz \right) + \frac{1}{2} \int \left(\sqrt{P_{XY}} - \sqrt{Q_{XY}} \right)^2 dx dy \\
 & = \mathbb{H}^2(P_{XY}, Q_{XY}) + \mathbb{H}^2(P_{YZ}, Q_{YZ})
 \end{aligned}$$

It remains to show the subadditivity with respect to product measures. If P, Q are product measures over X, Y , then $P_{XY} = P_X P_Y$ and $Q_{XY} = Q_X Q_Y$. Since all densities are non-negative, we have $\sqrt{P_Y Q_Y} \leq \frac{1}{2} (P_Y + Q_Y)$ point-wise. Hence,

$$\begin{aligned}
 & \mathbb{H}^2(P_{XY}, Q_{XY}) \\
 & = 1 - \int \sqrt{P_{XY} Q_{XY}} dx dy \\
 & = 1 - \int \sqrt{P_X Q_X} \left(\int \sqrt{P_Y Q_Y} dy \right) dx \\
 & = 1 - \int \frac{1}{2} (P_X + Q_X) \left(\int \sqrt{P_Y Q_Y} dy \right) dx + \int \frac{1}{2} \left(\sqrt{P_X} - \sqrt{Q_X} \right)^2 \left(\int \sqrt{P_Y Q_Y} dy \right) dx \\
 & \leq 1 - \left(\int \frac{1}{2} (P_X + Q_X) dx \right) \left(\int \sqrt{P_Y Q_Y} dy \right) + \int \frac{1}{2} \left(\sqrt{P_X} - \sqrt{Q_X} \right)^2 \left(\int \frac{1}{2} (P_Y + Q_Y) dy \right) dx \\
 & = 1 - \int \sqrt{P_Y Q_Y} dy + \int \frac{1}{2} \left(\sqrt{P_X} - \sqrt{Q_X} \right)^2 dx \\
 & = \mathbb{H}^2(P_X, Q_X) + \mathbb{H}^2(P_Y, Q_Y)
 \end{aligned}$$

□

A.3. Proof of Theorem 3

Proof. The subadditivity of KL-divergence is claimed in (Daskalakis & Pan, 2017) without proof. Here, we provide a proof for completeness.

Given Theorem 1, we only need to show the following:

1. For two Markov Chains P, Q on variables $X \rightarrow Y \rightarrow Z$, it holds that $\text{KL}(P_{XYZ}, Q_{XYZ}) \leq \text{KL}(P_{XY}, Q_{XY}) + \text{KL}(P_{YZ}, Q_{YZ})$.
2. For two product measures P, Q on variables X, Y , it holds that $\text{KL}(P_{XY}, Q_{XY}) \leq \text{KL}(P_X, Q_X) + \text{KL}(P_Y, Q_Y)$.

We first show the subadditivity with respect to Markov Chains. The Markov property implies $P_{XYZ} = P_{XY} P_{YZ} / P_Y$ (and the same holds for Q). Thus,

$$\begin{aligned}
 \text{KL}(P_{XYZ}, Q_{XYZ}) & = \int P_{XYZ} \log \left(\frac{P_{XY} P_{YZ}}{Q_{XY} Q_{YZ}} \frac{P_Y}{Q_Y} \right) dx dy dz \\
 & = \int P_{XY} \log \left(\frac{P_{XY}}{Q_{XY}} \right) dx dy + \int P_{YZ} \log \left(\frac{P_{YZ}}{Q_{YZ}} \right) dy dz - \int P_Y \log \left(\frac{P_Y}{Q_Y} \right) dy \\
 & = \text{KL}(P_{XY}, Q_{XY}) + \text{KL}(P_{YZ}, Q_{YZ}) - \text{KL}(P_Y, Q_Y)
 \end{aligned}$$

The subadditivity follows from the non-negativity of KL-divergence. Additivity holds when $\text{KL}(P_Y, Q_Y) = 0$.

It remains to show the subadditivity with respect to product measures. We will, in fact, show additivity rather than subadditivity. If P, Q are product measures over X, Y , then $P_{XY} = P_X P_Y$ and $Q_{XY} = Q_X Q_Y$, hence,

$$\begin{aligned} \text{KL}(P_{XY}, Q_{XY}) &= \int P_{XY} \log \left(\frac{P_X P_Y}{Q_X Q_Y} \right) dx dy \\ &= \int P_X \log \left(\frac{P_X}{Q_X} \right) dx + \int P_Y \log \left(\frac{P_Y}{Q_Y} \right) dy \\ &= \text{KL}(P_X, Q_X) + \text{KL}(P_Y, Q_Y). \end{aligned}$$

□

A.4. Proof of Corollary 5

Proof. The subadditivity of Jensen-Shannon divergence follows from:

1. The subadditivity of squared Hellinger distance (Theorem 2).
2. f -Divergence inequalities (Theorem 11 of (Sason & Verdu, 2016), repeated as Theorem 17 in Appendix B.2): For any two densities P and Q ,

$$(\ln 2)H^2(P, Q) \leq \text{JS}(P, Q) \leq H^2(P, Q)$$

Combining the inequalities implies that, for any pair of Bayes-nets P, Q with respect to a DAG G , we have,

$$\text{JS}(P, Q) \leq H^2(P, Q) \leq \sum_{i=1}^n H^2(P_{\Pi_i \cup X_i}, Q_{\Pi_i \cup X_i}) \leq \frac{1}{\ln 2} \sum_{i=1}^n \text{JS}(P_{\Pi_i \cup X_i}, Q_{\Pi_i \cup X_i})$$

This proves that Jensen-Shannon divergence satisfies $\ln 2$ -linear subadditivity on Bayes-nets.

Note that we assume natural logarithm is used in the definition of Jensen-Shannon divergence when deriving the inequalities between $\text{JS}(P, Q)$ and $H^2(P, Q)$ (see Theorem 17 for details). However, the choice of the base of the logarithm does not affect the $\ln 2$ -linear subadditivity of Jensen-Shannon divergence. □

A.5. Proof of Theorem 6

In the following proofs, we extensively use the Integral Probability Metric (IPM) formula of Total Variation distance (Müller, 1997). If \mathcal{F} is the set of measurable functions on Ω taking values in $[0, 1]$, then,

$$\text{TV}(P, Q) = \sup_{\phi \in \mathcal{F}} \left| \mathbb{E}_{x \sim P}[\phi(x)] - \mathbb{E}_{x \sim Q}[\phi(x)] \right|$$

Lemma 12. *Let P and Q be two Bayes-nets with respect to DAG $X \rightarrow Y \rightarrow Z$. Then,*

$$\text{TV}(P_{XYZ}, Q_{XYZ}) \leq \text{TV}(P_{XY}, Q_{XY}) + \text{TV}(P_Y, Q_Y) + \text{TV}(P_{YZ}, Q_{YZ})$$

Proof. We do a hybrid argument. By the triangle inequality, we have:

$$\text{TV}(P_{XYZ}, Q_{XYZ}) \leq \text{TV}(P_{XYZ}, P_{XY}Q_{Z|Y}) + \text{TV}(P_{XY}Q_{Z|Y}, Q_{XYZ})$$

We bound each term on the right-hand side separately.

Let us start with the second term. Let \mathcal{F}_{xy} be the set of measurable functions on variables x and y taking values in $[0, 1]$, and \mathcal{F}_{xyz} be the set of measurable functions on variables x, y, z taking values in $[0, 1]$, etc. Using the Markov property, we know $P_{XYZ} = P_{XY}P_{Z|Y} = P_Y P_{X|Y} P_{Z|Y}$ (and the same holds for Q). Then,

$$\begin{aligned} \text{TV}(P_{XY}Q_{Z|Y}, Q_{XYZ}) &= \sup_{\phi \in \mathcal{F}_{xyz}} \left| \mathbb{E}_{P_{XY}Q_{Z|Y}}[\phi(x, y, z)] - \mathbb{E}_{Q_{XYZ}}[\phi(x, y, z)] \right| \\ &= \sup_{\phi \in \mathcal{F}_{xyz}} \left| \mathbb{E}_{P_{XY}} \left[\mathbb{E}_{Q_{Z|Y}}[\phi(x, y, z)] \right] - \mathbb{E}_{Q_{XY}} \left[\mathbb{E}_{Q_{Z|Y}}[\phi(x, y, z)] \right] \right| \\ &\leq \sup_{\phi \in \mathcal{F}_{xy}} \left| \mathbb{E}_{P_{XY}}[\phi(x, y)] - \mathbb{E}_{Q_{XY}}[\phi(x, y)] \right| \\ &\equiv \text{TV}(P_{XY}, Q_{XY}) \end{aligned}$$

Let us now bound the first term,

$$\begin{aligned}
 \text{TV}(P_{XYZ}, P_{XY}Q_{Z|Y}) &= \sup_{\phi \in \mathcal{F}_{xyz}} \left| \mathbb{E}_{P_{XYZ}}[\phi(x, y, z)] - \mathbb{E}_{P_{XY}Q_{Z|Y}}[\phi(x, y, z)] \right| \\
 &= \sup_{\phi \in \mathcal{F}_{xyz}} \left| \mathbb{E}_{P_Y P_{Z|Y}} \left[\mathbb{E}_{P_{X|Y}}[\phi(x, y, z)] \right] - \mathbb{E}_{P_Y Q_{Z|Y}} \left[\mathbb{E}_{P_{X|Y}}[\phi(x, y, z)] \right] \right| \\
 &\leq \sup_{\phi \in \mathcal{F}_{yz}} \left| \mathbb{E}_{P_Y P_{Z|Y}}[\phi(y, z)] - \mathbb{E}_{P_Y Q_{Z|Y}}[\phi(y, z)] \right| \\
 &\leq \sup_{\phi \in \mathcal{F}_{yz}} \left| \mathbb{E}_{P_Y P_{Z|Y}}[\phi(y, z)] - \mathbb{E}_{Q_Y Q_{Z|Y}}[\phi(y, z)] \right| + \sup_{\phi \in \mathcal{F}_{yz}} \left| \mathbb{E}_{Q_Y Q_{Z|Y}}[\phi(y, z)] - \mathbb{E}_{P_Y Q_{Z|Y}}[\phi(y, z)] \right| \\
 &= \text{TV}(P_{YZ}, Q_{YZ}) + \sup_{\phi \in \mathcal{F}_{yz}} \left| \mathbb{E}_{Q_Y} \left[\mathbb{E}_{Q_{Z|Y}}[\phi(y, z)] \right] - \mathbb{E}_{P_Y} \left[\mathbb{E}_{Q_{Z|Y}}[\phi(y, z)] \right] \right| \\
 &\leq \text{TV}(P_{YZ}, Q_{YZ}) + \sup_{\phi \in \mathcal{F}_y} \left| \mathbb{E}_{Q_Y}[\phi(y)] - \mathbb{E}_{P_Y}[\phi(y)] \right| \\
 &\leq \text{TV}(P_{YZ}, Q_{YZ}) + \text{TV}(P_Y, Q_Y)
 \end{aligned}$$

Combining the two inequalities concludes the proof. \square

Lemma 13. *Let P and Q be two product measures over variables X and Y . Then,*

$$\text{TV}(P_{XY}, Q_{XY}) \leq \text{TV}(P_X, Q_X) + \text{TV}(P_Y, Q_Y)$$

Proof. By the triangle inequality, we have:

$$\text{TV}(P_{XY}, Q_{XY}) \leq \text{TV}(P_{XY}, P_X Q_Y) + \text{TV}(P_X Q_Y, Q_{XY})$$

We bound each term on the right hand side separately. Let \mathcal{F}_{xy} be the set of measurable functions on variables x and y taking values in $[0, 1]$, and \mathcal{F}_y be the set of measurable functions on variable y taking values in $[0, 1]$, etc. Then,

$$\begin{aligned}
 \text{TV}(P_{XY}, P_X Q_Y) &= \sup_{\phi \in \mathcal{F}_{xy}} \left| \mathbb{E}_{P_{XY}}[\phi(x, y)] - \mathbb{E}_{P_X Q_Y}[\phi(x, y)] \right| \\
 &= \sup_{\phi \in \mathcal{F}_{xy}} \left| \mathbb{E}_{P_Y} \left[\mathbb{E}_{P_X}[\phi(x, y)] \right] - \mathbb{E}_{Q_Y} \left[\mathbb{E}_{P_X}[\phi(x, y)] \right] \right| \\
 &\leq \sup_{\phi \in \mathcal{F}_y} \left| \mathbb{E}_{P_Y}[\phi(y)] - \mathbb{E}_{Q_Y}[\phi(y)] \right| \\
 &\equiv \text{TV}(P_Y, Q_Y)
 \end{aligned}$$

Similarly, we get $\text{TV}(P_X Q_Y, Q_{XY}) \leq \text{TV}(P_X, Q_X)$. Combining the two inequalities concludes the proof. \square

Proof of Theorem 6: Similar to the proof of Theorem 1, for a pair of Bayes-nets P and Q with respect to a DAG G , we perform induction on each nodes of G . Consider the topological ordering $(1, \dots, n)$ of the nodes of G . Consistent with the topological ordering, consider the following Markov Chain on super-nodes: $X_{\{1, \dots, n-1\} \setminus \Pi_n} \rightarrow X_{\Pi_n} \rightarrow X_n$, where Π_n is the set of parents of node n and $\Pi_n \subseteq \{1, \dots, n-1\}$. We distinguish three cases:

- $\Pi_n \neq \emptyset$ and $\Pi_n \subsetneq \{1, \dots, n-1\}$: In this case, we apply Lemma 12 to get $\text{TV}(P, Q) \leq \text{TV}(P_{\cup_{i=1}^{n-1} X_i}, Q_{\cup_{i=1}^{n-1} X_i}) + \text{TV}(P_{X_{\Pi_n}}, Q_{X_{\Pi_n}}) + \text{TV}(P_{X_{\Pi_n} \cup X_n}, Q_{X_{\Pi_n} \cup X_n})$.
- $\Pi_n = \{1, \dots, n-1\}$: In this case, it is trivial that $\text{TV}(P, Q) \equiv \text{TV}(P_{X_{\Pi_n} \cup X_n}, Q_{X_{\Pi_n} \cup X_n}) \leq \text{TV}(P_{\cup_{i=1}^{n-1} X_i}, Q_{\cup_{i=1}^{n-1} X_i}) + \text{TV}(P_{X_{\Pi_n}}, Q_{X_{\Pi_n}}) + \text{TV}(P_{X_{\Pi_n} \cup X_n}, Q_{X_{\Pi_n} \cup X_n})$.
- $\Pi_n = \emptyset$: In this case, X_n is independent from (X_1, \dots, X_{n-1}) in both Bayes-nets. Thus we apply Lemma 13 to get $\text{TV}(P, Q) \leq \text{TV}(P_{\cup_{i=1}^{n-1} X_i}, Q_{\cup_{i=1}^{n-1} X_i}) + \text{TV}(P_{X_n}, Q_{X_n}) \equiv \text{TV}(P_{\cup_{i=1}^{n-1} X_i}, Q_{\cup_{i=1}^{n-1} X_i}) + \text{TV}(P_{X_{\Pi_n}}, Q_{X_{\Pi_n}}) + \text{TV}(P_{X_{\Pi_n} \cup X_n}, Q_{X_{\Pi_n} \cup X_n})$, where $\text{TV}(P_{X_{\Pi_n}}, Q_{X_{\Pi_n}}) = 0$ and $\text{TV}(P_{X_{\Pi_n} \cup X_n}, Q_{X_{\Pi_n} \cup X_n}) = \text{TV}(P_{X_1}, Q_{X_1})$ as $\Pi_n = \emptyset$.

We proceed by induction. For each inductive step $k = 1, \dots, n-2$, we consider the following Markov Chain on super-nodes: $X_{\{1, \dots, n-k-1\} \setminus \Pi_{n-k}} \rightarrow X_{\Pi_{n-k}} \rightarrow X_{n-k}$. No matter what Π_{n-k} is, we always have: $\text{TV}(P_{\cup_{i=1}^{n-k} X_i}, Q_{\cup_{i=1}^{n-k} X_i}) \leq \text{TV}(P_{\cup_{i=1}^{n-k-1} X_i}, Q_{\cup_{i=1}^{n-k-1} X_i}) + \text{TV}(P_{X_{\Pi_{n-k}}}, Q_{X_{\Pi_{n-k}}}) + \text{TV}(P_{X_{\Pi_{n-k}} \cup X_{n-k}}, Q_{X_{\Pi_{n-k}} \cup X_{n-k}})$. In the end of the induction, we obtain: $\text{TV}(P, Q) \leq \text{TV}(P_{X_1}, Q_{X_1}) + \sum_{i=2}^n (\text{TV}(P_{\Pi_i \cup X_i}, Q_{\Pi_i \cup X_i}) + \text{TV}(P_{\Pi_i}, Q_{\Pi_i}))$. Since $\Pi_1 \equiv \emptyset$, we know $\text{TV}(P_{X_{\Pi_1}}, Q_{X_{\Pi_1}}) = 0$ and $\text{TV}(P_{X_{\Pi_1} \cup X_1}, Q_{X_{\Pi_1} \cup X_1}) = \text{TV}(P_{X_1}, Q_{X_1})$. Hence, we conclude that,

$$\text{TV}(P, Q) \leq \sum_{i=1}^n \left(\text{TV}(P_{\Pi_i \cup X_i}, Q_{\Pi_i \cup X_i}) + \text{TV}(P_{\Pi_i}, Q_{\Pi_i}) \right)$$

Now we relate this inequality to the notion of linear subadditivity. For two densities P and Q on variables X, Y , it holds that,

$$\begin{aligned} \text{TV}(P_X, Q_X) &\equiv \frac{1}{2} \int |P_X - Q_X| dx \\ &= \frac{1}{2} \int \left| \int P_{XY} dy - \int Q_{XY} dy \right| dx \\ &\leq \frac{1}{2} \int \left(\int |P_{XY} - Q_{XY}| dy \right) dx \\ &\equiv \text{TV}(P_{XY}, Q_{XY}) \end{aligned}$$

Applying this inequality to X_{Π_i} and X_i , for any $i \in \{1, \dots, n\}$, we obtain, $\text{TV}(P_{\Pi_i}, Q_{\Pi_i}) \leq \text{TV}(P_{\Pi_i \cup X_i}, Q_{\Pi_i \cup X_i})$. Thus,

$$\text{TV}(P, Q) \leq 2 \sum_{i=1}^n \text{TV}(P_{\Pi_i \cup X_i}, Q_{\Pi_i \cup X_i})$$

This concludes that Total Variation distance satisfies $\frac{1}{2}$ -linear subadditivity on Bayes-nets. \square

A.6. Proof of Theorem 8

Proof. For reference, we repeat the three conditions of the IPM subadditivity upper-bound here:

- (1) The space Ω is bounded, i.e. $\text{diam}(\Omega) < \infty$.
- (2) Each discriminator class \mathcal{F}_i is larger than the set of neural networks with a single neuron, which have ReLU activation and bounded parameters, i.e. for any $i \in \{1, \dots, n\}$, we have $\mathcal{F}_i \supseteq \{\max\{w^T x + b, 0\} | w \in \mathbb{R}^{nd}, b \in \mathbb{R}, \|[w, b]\|_2 = 1\}$.
- (3) For any $i \in \{1, \dots, n\}$, $\log(P_{X_i \cup X_{\Pi_i}}/Q_{X_i \cup X_{\Pi_i}})$ exists, and is bounded and Lipschitz continuous.

For two distributions P, Q and a set of discriminators \mathcal{F} satisfying all the three conditions, by Theorem 24 we know that for any $i \in \{1, \dots, n\}$, $\log(P_{X_i \cup X_{\Pi_i}}/Q_{X_i \cup X_{\Pi_i}})$ is inside the closure of the linear span of \mathcal{F}_i , i.e. $\log(P_{X_i \cup X_{\Pi_i}}/Q_{X_i \cup X_{\Pi_i}}) \in \text{cl}(\text{span} \mathcal{F}_i)$. Moreover, $\log(P_{X_i \cup X_{\Pi_i}}/Q_{X_i \cup X_{\Pi_i}})$ is approximated by \mathcal{F}_i with an error decay function, denoted by $\varepsilon_i(r)$. Using Theorem 23, we upper-bound the Jeffrey divergence between local marginals, $\text{JF}(P_{X_i \cup X_{\Pi_i}}, Q_{X_i \cup X_{\Pi_i}})$, by a set of linear functions of the corresponding IPM $d_{\mathcal{F}}(P_{X_i \cup X_{\Pi_i}}, Q_{X_i \cup X_{\Pi_i}})$,

$$\text{JF}(P_{X_i \cup X_{\Pi_i}}, Q_{X_i \cup X_{\Pi_i}}) \leq 2\varepsilon_i(r) + r d_{\mathcal{F}}(P_{X_i \cup X_{\Pi_i}}, Q_{X_i \cup X_{\Pi_i}}) \quad \forall r \geq 0, \forall i \in \{1, \dots, n\}$$

Because of the condition (3): $\log(P_{X_i \cup X_{\Pi_i}}/Q_{X_i \cup X_{\Pi_i}})$ is bounded and Lipschitz continuous, for any $i \in \{1, \dots, n\}$, there exists a constant $\eta_i > 0$, such that,

$$\left\| \log(P_{X_i \cup X_{\Pi_i}}/Q_{X_i \cup X_{\Pi_i}}) \right\|_{\infty} < \eta_i$$

and for any $x, y \in \Omega_{X_i \cup X_{\Pi_i}}$ (which is the space of variables $X_i \cup X_{\Pi_i}$), it holds that,

$$\left\| \log(P_{X_i \cup X_{\Pi_i}}(x)/Q_{X_i \cup X_{\Pi_i}}(x)) - \log(P_{X_i \cup X_{\Pi_i}}(y)/Q_{X_i \cup X_{\Pi_i}}(y)) \right\|_{\infty} \leq \frac{\eta_i}{\text{diam}(\Omega_{X_i \cup X_{\Pi_i}})} \|x - y\|_2$$

Again, by Theorem 24, we get an efficient upper-bound on $\varepsilon_i(r)$,

$$\varepsilon_i(r) \leq C_i(nd) \eta_i \left(\frac{r}{\eta_i} \right)^{-\frac{2}{nd+1}} \log \left(\frac{r}{\eta_i} \right) \quad \forall r \geq R_i(nd), \forall i \in \{1, \dots, n\}$$

where $C_i(nd)$ and $R_i(nd)$ are constants that only depend on the number of dimensions, nd .

Since all error decay functions $\varepsilon_i(r)$ are monotonically decreasing with respect to r . We can choose an absolute constant $\epsilon_0 > 0$. Let r_i^* be the smallest r such that $\varepsilon_i(r_i^*) \leq \epsilon_0$, i.e. for any $i \in \{1, \dots, n\}$, define $r_i^* = \inf\{r | \varepsilon_i(r) \leq \epsilon_0\}$. Fix this r_i^* for the upper-bound on $\text{JF}(P_{X_i \cup X_{\Pi_i}}, Q_{X_i \cup X_{\Pi_i}})$, we obtain,

$$\text{JF}(P_{X_i \cup X_{\Pi_i}}, Q_{X_i \cup X_{\Pi_i}}) \leq 2\epsilon_0 + r_i^* d_{\mathcal{F}}(P_{X_i \cup X_{\Pi_i}}, Q_{X_i \cup X_{\Pi_i}}) \quad \forall i \in \{1, \dots, n\}$$

The upper bound on $\varepsilon_i(r)$, i.e. $C_i(nd)\eta_i (r/\eta_i)^{-\frac{2}{nd+1}} \log(r/\eta_i)$ is a monotonically decreasing function, if r is larger than a constant that only depends on η_i and the dimensionality nd , denoted by $R_i^*(\eta_i, nd)$. In such case, we have,

$$r_i^* \leq \inf \left\{ r \mid C_i(nd)\eta_i \left(\frac{r}{\eta_i} \right)^{-\frac{2}{nd+1}} \log \left(\frac{r}{\eta_i} \right) \leq \epsilon_0, \text{ and } r \geq \max \{R_i(nd), R_i^*(\eta_i, nd)\} \right\} \quad \forall i \in \{1, \dots, n\}$$

If we define,

$$r_0(\epsilon_0, \boldsymbol{\eta}, nd) := \max_{i \in \{1, \dots, n\}} \left\{ \inf \left\{ r \mid C_i(nd)\eta_i \left(\frac{r}{\eta_i} \right)^{-\frac{2}{nd+1}} \log \left(\frac{r}{\eta_i} \right) \leq \epsilon_0, \text{ and } r \geq \max \{R_i(nd), R_i^*(\eta_i, nd)\} \right\} \right\}$$

where $\boldsymbol{\eta} = [\eta_1, \dots, \eta_n]$ is the tuple of η_i . Then clearly,

$$r_i^* \leq r_0(\epsilon_0, \boldsymbol{\eta}, nd) \quad \forall i \in \{1, \dots, n\}$$

Hence, we can further relax the upper-bound on $\text{JF}(P_{X_i \cup X_{\Pi_i}}, Q_{X_i \cup X_{\Pi_i}})$ to a linear function of $d_{\mathcal{F}}(P_{X_i \cup X_{\Pi_i}}, Q_{X_i \cup X_{\Pi_i}})$ with a constant coefficient,

$$\text{JF}(P_{X_i \cup X_{\Pi_i}}, Q_{X_i \cup X_{\Pi_i}}) \leq 2\epsilon_0 + r_0(\epsilon_0, \boldsymbol{\eta}, nd) d_{\mathcal{F}}(P_{X_i \cup X_{\Pi_i}}, Q_{X_i \cup X_{\Pi_i}}) \quad \forall i \in \{1, \dots, n\}$$

Where ϵ_0 is an absolute constant, and $r_0(\epsilon_0, \boldsymbol{\eta}, nd)$ is independent of the distributions P, Q and all the sets of discriminators $\mathcal{F} = [\mathcal{F}_1, \dots, \mathcal{F}_n]$. It is a uniform upper-bound on all Jeffrey divergences between local marginals.

Summing up the inequalities for all $i \in \{1, \dots, n\}$. Because of the subadditivity of Jeffrey divergence on Bayes-nets P and Q (Corollary 4), we get,

$$\frac{\text{JF}(P, Q)}{r_0(\epsilon_0, \boldsymbol{\eta}, nd)} - \frac{2n\epsilon_0}{r_0(\epsilon_0, \boldsymbol{\eta}, nd)} \leq \sum_{i=1}^n d_{\mathcal{F}}(P_{X_i \cup X_{\Pi_i}}, Q_{X_i \cup X_{\Pi_i}})$$

Moreover, by the inequality $W_1(P, Q) \leq \text{diam}(\Omega) \text{TV}(P, Q)$ (a special case of Theorem 21) for bounded space Ω (condition (1)), and the Pinsker's inequality $\text{TV}(P, Q) \leq \sqrt{\frac{1}{2} \text{KL}(P, Q)}$ (Theorem 18), we have,

$$\frac{4}{\text{diam}(\Omega)^2} W_1^2(P, Q) \leq 4 \text{TV}^2(P, Q) \leq \text{JF}(P, Q)$$

Combining the two inequalities, we finally conclude that,

$$\frac{4}{r_0(\epsilon_0, \boldsymbol{\eta}, nd) \text{diam}(\Omega)^2} W_1^2(P, Q) - \frac{2n\epsilon_0}{r_0(\epsilon_0, \boldsymbol{\eta}, nd)} \leq \sum_{i=1}^n d_{\mathcal{F}}(P_{X_i \cup X_{\Pi_i}}, Q_{X_i \cup X_{\Pi_i}})$$

This means that the sum of IPMs between the local marginals $\sum_{i=1}^n d_{\mathcal{F}}(P_{X_i \cup X_{\Pi_i}}, Q_{X_i \cup X_{\Pi_i}})$ (we call it the IPM subadditivity upper-bound) can upper bound the squared 1-Wasserstein distance $W_1^2(P, Q)$ up to some constant coefficient,

$$\alpha = \frac{4}{r_0(\epsilon_0, \boldsymbol{\eta}, nd) \text{diam}(\Omega)^2}$$

and additive error,

$$\epsilon = \frac{2n\epsilon_0}{r_0(\epsilon_0, \boldsymbol{\eta}, nd)}$$

independent of the distributions P, Q and all the sets of discriminators $\mathcal{F} = [\mathcal{F}_1, \dots, \mathcal{F}_n]$. \square

A.7. Proof of Theorem 9

Lemma 14. For two-sided ϵ -close distributions P, Q with $\epsilon \rightarrow 0$, any f -divergence $D_f(P, Q)$ with $f(t)$ twice differentiable at $t = 1$ and $f''(1) > 0$, is proportional to $\chi^2(P, Q)$ up to $\mathcal{O}(\epsilon^3)$, i.e.

$$D_f(P, Q) = \frac{f''(1)}{2} \chi^2(P, Q) + \mathcal{O}(\epsilon^3)$$

And χ^2 is now symmetric up to $\mathcal{O}(\epsilon^3)$, i.e. $\chi^2(P, Q) = \chi^2(Q, P) + \mathcal{O}(\epsilon^3)$.

Proof. Since $f(t)$ twice differentiable at $t = 1$, and $P(x)/Q(x) \in (1 - \epsilon, 1 + \epsilon)$ with $0 < \epsilon \ll 1$, by Taylor's theorem we get,

$$f\left(\frac{P}{Q}\right) = f'(1) \left(\frac{P}{Q} - 1\right) + \frac{1}{2} f''(1) \left(\frac{P}{Q} - 1\right)^2 + \mathcal{O}(\epsilon^3)$$

Multiply by Q and integrate over $\Omega \in \mathbb{R}^{nd}$ gives,

$$\begin{aligned} D_f(P, Q) &= \frac{f''(1)}{2} \int Q \left(\frac{P}{Q} - 1\right)^2 dx + \mathcal{O}(\epsilon^3) \\ &= \frac{f''(1)}{2} \chi^2(P, Q) + \mathcal{O}(\epsilon^3) \end{aligned}$$

Where the first order term vanishes because $\int P dx = \int Q dx = 1$. This equation implies that all f -divergences such that $f''(1) > 0$ behave similarly when the two distributions P and Q are sufficiently close.

Meanwhile, because $P/Q = 1 + \mathcal{O}(\epsilon)$, we have,

$$\begin{aligned} \chi^2(P, Q) &= \int \frac{(P - Q)^2}{P} \frac{P}{Q} dx \\ &= \int \frac{(P - Q)^2}{P} (1 + \mathcal{O}(\epsilon)) dx \\ &= \chi^2(Q, P) + \mathcal{O}(\epsilon^3) \end{aligned}$$

Thus we can exchange P and Q freely in any $\mathcal{O}(\epsilon^2)$ terms (e.g. $(P - Q)^2/Q$), while preserving the equality up to $\mathcal{O}(\epsilon^3)$. \square

Proof of Theorem 9: We first prove that the subadditivity inequality holds using Lemma 14. Define $R(x) = \frac{1}{2} \left(\sqrt{PQ} + \frac{P+Q}{2} \right)$ as the average of the geometric and arithmetic means of P and Q . Clearly for any $x \in \Omega$, it holds that $|R(x) - Q(x)| < |P(x) - Q(x)| < \epsilon$. Thus $R/Q = 1 + \mathcal{O}(\epsilon)$, and by Lemma 14, we have,

$$\begin{aligned} D_f(P, Q) &= \frac{f''(1)}{2} \chi^2(P, Q) + \mathcal{O}(\epsilon^3) \\ &= \frac{f''(1)}{2} \int \frac{(P - Q)^2}{R} \frac{R}{Q} dx + \mathcal{O}(\epsilon^3) \\ &= \frac{f''(1)}{2} \int \frac{(P - Q)^2}{R} dx + \mathcal{O}(\epsilon^3) \\ &= 2f''(1) \int \left(\sqrt{P} - \sqrt{Q} \right) dx + \mathcal{O}(\epsilon^3) \\ &= 4f''(1) H^2(P, Q) + \mathcal{O}(\epsilon^3) \end{aligned}$$

Since $f''(1) > 0$, we can re-write this equation as $H^2(P, Q) = \frac{1}{4f''(1)} D_f(P, Q) + \mathcal{O}(\epsilon^3)$. Applying this formula to both sides of the subadditivity inequality of H^2 (Theorem 2): $H^2(P, Q) \leq \sum_{i=1}^n H^2(P_{X_i \cup X_{\Pi_i}}, Q_{X_i \cup X_{\Pi_i}})$, we conclude that the subadditivity inequality holds up to $\mathcal{O}(\epsilon^3)$:

$$D_f(P, Q) \leq \sum_{i=1}^n D_f(P_{X_i \cup X_{\Pi_i}}, Q_{X_i \cup X_{\Pi_i}}) + \mathcal{O}(\epsilon^3)$$

Then, we prove that the subadditivity gap $\Delta := \sum_{i=1}^n D_f(P_{X_i \cup X_{\Pi_i}}, Q_{X_i \cup X_{\Pi_i}}) - D_f(P, Q)$ is proportional to $\sum_{i=1}^n \chi^2(P_{\Pi_i}, Q_{\Pi_i})$ up to $\mathcal{O}(\epsilon^3)$ using a different approach. Let us start from the simple case when P, Q are Markov Chains with structure $X \rightarrow Y \rightarrow Z$. The Markov property $P_{Z|XY} = P_{Z|Y}$ holds (and the same for Q). Since the joint distributions P_{XYZ} and Q_{XYZ} are two-sided ϵ -close, so are the marginal and conditional distributions. We define the differences between the marginals and conditionals of P and Q as follows,

$$\begin{aligned} Q_{X|Y} &= P_{X|Y} + \epsilon J_{X|Y} \\ Q_Y &= P_Y + \epsilon J_Y \\ Q_{Z|Y} &= P_{Z|Y} + \epsilon J_{Z|Y} \end{aligned}$$

Clearly $\int J_{X|Y} dx = \int J_Y dy = \int J_{Z|Y} dz = 0$. Using Lemma 14, we have,

$$\begin{aligned} & \frac{2}{\epsilon^2 f''(1)} D_f(P_{XYZ}, Q_{XYZ}) + \mathcal{O}(\epsilon) \\ &= \frac{1}{\epsilon^2} \int \frac{(P_{XYZ} - Q_{XYZ})^2}{P_{XYZ}} dx dy dz \\ &= \frac{1}{\epsilon^2} \int \frac{(P_{X|Y} P_Y P_{Z|Y} - Q_{X|Y} Q_Y Q_{Z|Y})^2}{P_{X|Y} P_Y P_{Z|Y}} dx dy dz \\ &= \int \left(\frac{J_Y^2 P_{X|Y} P_{Z|Y}}{P_Y} + \frac{J_{X|Y}^2 P_Y P_{Z|Y}}{P_{X|Y}} + \frac{J_{Z|Y}^2 P_{X|Y} P_Y}{P_{Z|Y}} + 2J_{X|Y} J_Y P_{Z|Y} + 2J_Y J_{Z|Y} P_{X|Y} + 2J_{X|Y} J_{Z|Y} P_Y \right) dx dy dz \\ &= \int \frac{J_Y^2}{P_Y} dy + \int \frac{J_{X|Y}^2 P_Y}{P_{X|Y}} dx dy + \int \frac{J_{Z|Y}^2 P_Y}{P_{Z|Y}} dy dz \end{aligned}$$

Similarly,

$$\begin{aligned} \frac{2}{\epsilon^2 f''(1)} D_f(P_{XY}, Q_{XY}) + \mathcal{O}(\epsilon) &= \frac{1}{\epsilon^2} \int \frac{(P_{X|Y} P_Y - Q_{X|Y} Q_Y)^2}{P_{X|Y} P_Y} dx dy \\ &= \int \left(\frac{J_{X|Y}^2 P_Y}{P_{X|Y}} + \frac{J_Y^2 P_{X|Y}}{P_Y} + 2J_{X|Y} J_Y \right) dx dy \\ &= \int \frac{J_{X|Y}^2 P_Y}{P_{X|Y}} dx dy + \int \frac{J_Y^2}{P_Y} dy \end{aligned}$$

And,

$$\frac{2}{\epsilon^2 f''(1)} D_f(P_{YZ}, Q_{YZ}) + \mathcal{O}(\epsilon) = \int \frac{J_{Z|Y}^2 P_Y}{P_{Z|Y}} dy dz + \int \frac{J_Y^2}{P_Y} dy$$

Thus, the subadditivity gap on the Markov Chain $X \rightarrow Y \rightarrow Z$ is,

$$\begin{aligned} \Delta_{\text{Markov Chain}} &= D_f(P_{XY}, Q_{XY}) + D_f(P_{YZ}, Q_{YZ}) - D_f(P_{XYZ}, Q_{XYZ}) \\ &= \frac{f''(1)}{2} \int \frac{J_Y^2}{P_Y} dy + \mathcal{O}(\epsilon^3) \\ &= \frac{f''(1)}{2} \chi^2(P_Y, Q_Y) + \mathcal{O}(\epsilon^3) \end{aligned}$$

Moreover, consider the special case when $Y = \emptyset$, thus P, Q are product measures on conditionally independent variables X and Z . Similarly, we have,

$$\frac{2}{\epsilon^2 f''(1)} D_f(P_{XZ}, Q_{XZ}) + \mathcal{O}(\epsilon) = \chi^2(P_X, Q_X) + \chi^2(P_Z, Q_Z)$$

Hence the subadditivity gap is,

$$\Delta_{\text{Product Measure}} = D_f(P_X, Q_X) + D_f(P_Z, Q_Z) - D_f(P_{XZ}, Q_{XZ}) = 0 + \mathcal{O}(\epsilon^3)$$

Now, for any pair of generic Bayes-nets P and Q , following the approach in the proof of Theorem 1 in Appendix A.1, we repeatedly apply the subadditivity inequality on Markov Chains of super-nodes $X_{\{1, \dots, n-k-1\} \setminus \Pi_{n-k}} \rightarrow X_{\Pi_{n-k}} \rightarrow X_{n-k}$, for $k = 0, 1, \dots, n-2$. Consider three cases:

- $\Pi_{n-k} \neq \emptyset$ and $\Pi_{n-k} \subsetneq \{1, \dots, n-k-1\}$: In this case, the subadditivity gap is $\frac{f''(1)}{2} \chi^2(P_{\Pi_{n-k}}, Q_{\Pi_{n-k}}) + \mathcal{O}(\epsilon^3)$.
- $\Pi_{n-k} = \{1, \dots, n-k-1\}$: In this case, as discussed in Appendix A.1, we add a redundant term $\delta(P_{\cup_{i=1}^{n-k-1} X_i}, Q_{\cup_{i=1}^{n-k-1} X_i}) \equiv \delta(P_{\Pi_{n-k}}, Q_{\Pi_{n-k}})$ into the subadditivity upper-bound. Thus, by Lemma 14, the subadditivity gap is $\frac{f''(1)}{2} \chi^2(P_{\Pi_{n-k}}, Q_{\Pi_{n-k}}) + \mathcal{O}(\epsilon^3)$
- $\Pi_{n-k} = \emptyset$: In this case, X_{n-k} is independent from (X_1, \dots, X_{n-k-1}) in both Bayes-nets. Thus the subadditivity gap is 0.

For all the three cases, the subadditivity gap at an induction step k is $\frac{f''(1)}{2} \chi^2(P_{\Pi_{n-k}}, Q_{\Pi_{n-k}}) + \mathcal{O}(\epsilon^3)$ (note that $\chi^2(P_{\Pi_{n-k}}, Q_{\Pi_{n-k}}) = 0$ when $\Pi_{n-k} = \emptyset$). Along with the induction process for $k = 0, 1, \dots, n-2$, the subadditivity gaps accumulate, and we finally get,

$$\Delta := \sum_{i=1}^n D_f(P_{X_i \cup X_{\Pi_i}}, Q_{X_i \cup X_{\Pi_i}}) - D_f(P, Q) = \frac{f''(1)}{2} \sum_{i=1}^n \chi^2(P_{\Pi_i}, Q_{\Pi_i}) + \mathcal{O}(\epsilon^3)$$

□

A.8. Proofs of Theorem 10 and Theorem 11

Lemma 15. Consider two f -divergences D_{f_1} and D_{f_2} with generator functions $f_1(t)$ and $f_2(t)$, where f_2 has subadditivity on Bayes-nets with respect to Definition 1. Let $I \subseteq (0, \infty)$ be an interval. If there exists two positive constants $A < B$, such that for any $t \in I$, it holds that $f_2(t) \geq 0$ and $A \leq f_1(t)/f_2(t) \leq B$. Then, for any pair of distributions P and Q , such that for any $x \in \Omega$, $P(x)/Q(x) \in I$, the linear subadditivity inequality of D_{f_1} holds with coefficient $0 < \alpha = A/B < 1$.

Proof. For any $t \in I$, multiplying $f_2(t) \geq 0$ to the inequalities $A \leq f_1(t)/f_2(t) \leq B$ gives,

$$A f_2(t) \leq f_1(t) \leq B f_2(t) \quad \forall t \in I$$

Similar to the proof of Lemma 16 in Appendix B.2, since for any $x \in \Omega$, it holds that $P(x)/Q(x) \in I$, we have,

$$A f_2(P(x)/Q(x)) \leq f_1(P(x)/Q(x)) \leq B f_2(P(x)/Q(x)) \quad \forall x \in \Omega$$

Multiply non-negative $Q(x)$ and integrate over Ω . Thus, for such pairs of P, Q , we obtain,

$$A D_{f_2}(P, Q) \leq D_{f_1}(P, Q) \leq B D_{f_2}(P, Q)$$

Now consider P, Q are Bayes-nets such that for any $x \in \Omega$, $P(x)/Q(x) \in I = [a, b]$, i.e. $a \leq P(x)/Q(x) \leq b$. For any non-empty set $S \subsetneq \{X_1, \dots, X_n\}$, let $\Omega_{\{X_1, \dots, X_n\} \setminus S}$ be the space of the variables not in S . Then, multiplying non-negative $Q(x)$ to $a \leq P(x)/Q(x) \leq b$ and integrating over $\Omega_{\{X_1, \dots, X_n\} \setminus S}$ gives $a Q_S \leq P_S \leq b Q_S$. Moreover, Q_S is positive because Q is positive. Thus, for any pair of marginal distributions P_S and Q_S of such distributions, they also satisfy that for any $x \in \Omega_S$, $P_S(x)/Q_S(x) \in I = [a, b]$.

Applying the first inequality to pairs of marginals $P_{X_i \cup X_{\Pi_i}}$ and $Q_{X_i \cup X_{\Pi_i}}$ gives,

$$D_{f_2}(P_{X_i \cup X_{\Pi_i}}, Q_{X_i \cup X_{\Pi_i}}) \leq \frac{1}{A} D_{f_1}(P_{X_i \cup X_{\Pi_i}}, Q_{X_i \cup X_{\Pi_i}}) \quad \forall i \in \{1, \dots, n\}$$

Similarly, applying the second inequality to P and Q gives,

$$\frac{1}{B} D_{f_1}(P, Q) \leq D_{f_2}(P, Q)$$

Combine them with the subadditivity inequality of D_{f_2} , i.e. $D_{f_2}(P, Q) \leq \sum_{i=1}^n D_{f_2}(P_{X_i \cup X_{\Pi_i}}, Q_{X_i \cup X_{\Pi_i}})$, we have,

$$\frac{A}{B} D_{f_1}(P, Q) \leq \sum_{i=1}^n D_{f_1}(P_{X_i \cup X_{\Pi_i}}, Q_{X_i \cup X_{\Pi_i}})$$

This proves that D_{f_1} satisfy A/B -linear subadditivity for such pairs of Bayes-nets P and Q . □

Proof of Theorem 10: Following Lemma 15, we consider the quotient $f(t)/f_{\text{H}^2}(t)$, where f_{H^2} is the generator function of squared Hellinger distance, and $f_{\text{H}^2}(t) := \frac{1}{2}(\sqrt{t} - 1)^2 \geq 0$ is always non-negative. If we can bound this quotient by positive numbers on an interval $t \in (1 - \epsilon, 1 + \epsilon)$ for some $0 < \epsilon < 1$, then by Lemma 15, we prove that D_f satisfies linear subadditivity when the distributions P and Q are two-sided ϵ -close.

Because $f(t)$ and $f_{\text{H}^2}(t)$ are continuous functions on $(0, \infty)$, the quotient $f(t)/f_{\text{H}^2}(t)$ is also continuous on $(0, \infty)$. To bound the quotient in the neighborhood around $t = 1$, we need to prove $\lim_{t \rightarrow 1} f(t)/f_{\text{H}^2}(t)$ exists and is positive. For f_{H^2} , we know $f'_{\text{H}^2}(1) = \frac{1}{2}(1 - 1/\sqrt{t})|_{t=1} = 0$ and $f''_{\text{H}^2}(1) = \frac{1}{4}t^{-3/2}|_{t=1} = \frac{1}{4} > 0$. Thus, since $f(t)$ is twice differentiable at $t = 1$, the limit of the quotient at $t = 1$ exists and is positive if and only if $f'(1) = 0$ and $f''(1) > 0$. That is,

$$0 < \lim_{t \rightarrow 1} f(t)/f_{\text{H}^2}(t) < \infty \iff f'(1) = 0 \text{ and } f''(1) > 0$$

The latter condition is given, but the former condition, $f'(1) = 0$, does not hold even for some f -divergences which satisfy subadditivity on any Bayes-nets, e.g. for KL divergence, $f'_{\text{KL}}(1) = 1 + \log(t)|_{t=1} = 1 \neq 0$.

However a trick can be used to rewrite the generator function $f(t)$ without changing the definition of D_f , so that the modified generator function satisfies the desired condition. For any $k \in \mathbb{R}$, the modified generator $\hat{f}(t) = f(t) + k(t - 1)$ defines the same f -divergence,

$$D_{\hat{f}}(P, Q) = \int Q \hat{f}\left(\frac{P}{Q}\right) dx = \int Q \left(f\left(\frac{P}{Q}\right) + k\left(\frac{P}{Q} - 1\right) \right) dx = \int Q f\left(\frac{P}{Q}\right) dx + k \int (P - Q) dx = D_f(P, Q)$$

Thus, for any $f(t)$ twice differentiable at $t = 1$ with $f''(1) > 0$, we can define $\hat{f}(t) := f(t) - f'(1)(t - 1)$. It is easy to verify that $\hat{f}(t)$ has zero first derivative $\hat{f}'(1) = 0$ and positive second derivative $\hat{f}''(1) > 0$ at $t = 1$. The modified generator satisfies the two required conditions. As a consequence, we have $0 < \lim_{t \rightarrow 1} \hat{f}(t)/f_{\text{H}^2}(t) < \infty$, and the quotient can be bounded by positive numbers in the neighborhood of $t = 1$, because of the continuity of $f(t)$. Applying Lemma 15 to interval $I = (1 - \epsilon, 1 + \epsilon)$ concludes the proof. \square

Proof of Theorem 11: From the proof of Theorem 10, let $\hat{f}(t) := f(t) - f'(1)(t - 1)$ be the modified generator function. We know the quotient $\hat{f}(t)/f_{\text{H}^2}(t)$ can be bounded by positive numbers for any $t \in (1 - \epsilon, 1 + \epsilon)$ for some $0 < \epsilon < 1$. It remains to prove that $\hat{f}(t)/f_{\text{H}^2}(t)$ can be bounded by positive numbers on the interval $[0, 1 - \epsilon)$.

The generator $f(t)$ is a strictly convex function on $(0, \infty)$, so is the modified generator $\hat{f}(t)$, since their difference is a linear function of t . Because $\hat{f}'(1) = 0$, the tangent line of the curve of $\hat{f}(t)$ at $t = 1$ coincides with the x-axis. Since $\hat{f}(t)$ is strictly convex on $(0, \infty)$, the graph of $\hat{f}(t)$ lies above the x-axis, i.e. for any $t \in (0, \infty)$ we have $\hat{f}(t) \geq 0$, where the equality holds if and only if $t = 1$. Hence, for any $t \in [0, 1 - \epsilon)$, it holds that $\hat{f}(t) > 0$. Moreover, $\hat{f}(0) = f(0) + f'(1)$ and we know $f(0) = \lim_{t \downarrow 0} f(t)$ is finite. In this sense, $\hat{f}(0)$ is finite and positive. By the continuity of the modified generator $\hat{f}(t)$, we know $\hat{f}(t)$ can be bounded by positive numbers on $[0, 1 - \epsilon)$. Moreover, clearly $f_{\text{H}^2}(t) := \frac{1}{2}(\sqrt{t} - 1)^2$ can be bounded by positive numbers $[0, 1 - \epsilon)$. This implies that the quotient $\hat{f}(t)/f_{\text{H}^2}(t)$ can be bounded by positive numbers on $[0, 1 - \epsilon)$. Applying Lemma 15 to the combined interval $I = [0, 1 + \epsilon) = [0, 1 - \epsilon) \cup \{1\} \cup (1 - \epsilon, 1 + \epsilon)$ concludes the proof. \square

B. f -Divergences and Inequalities

B.1. Common f -Divergences

All commonly-used f -divergences are listed in Table 4.

Name	Notation	Generator $f(t)$
KullbackLeibler	KL	$t \log(t)$
Reverse KullbackLeibler	RKL	$-\log(t)$
Jeffrey	JF	$(t-1) \log(t)$
Jensen-Shannon	JS	$\frac{t}{2} \log \frac{2t}{t+1} + \frac{1}{2} \log \frac{2}{t+1}$
Squared Hellinger	H ²	$\frac{1}{2} (\sqrt{t} - 1)^2$
Total Variation	TV	$\frac{1}{2} t - 1 $
Pearson χ^2	χ^2	$(t-1)^2$
Reverse Pearson χ^2	$R\chi^2$	$\frac{1}{t} - t$
α -Divergence	\mathcal{H}_α	$\begin{cases} \frac{t^\alpha - 1}{\alpha(\alpha-1)} & \alpha \neq 0, 1 \\ t \ln t & \alpha = 1 \\ -\ln t & \alpha = 0 \end{cases}$

 Table 4. List of common f -divergences with generator functions.

We always adopt the most widely-accepted definitions. Note the $\frac{1}{2}$ coefficients in the definitions of squared Hellinger distance and Total Variation distance, in the spirit of normalizing their ranges to $[0, 1]$.

The α -divergences \mathcal{H}_α ($\alpha \in \mathbb{R}$), popularized by (Liese & Vajda, 2006), generalize many f -divergences including KL divergence, reverse KL divergence, χ^2 divergence, reverse χ^2 divergence, and Hellinger distances. More specifically, we have the following relations: $\mathcal{H}_1 = \text{KL}$, $\mathcal{H}_0 = \text{RKL}$, $\mathcal{H}_2 = \frac{1}{2}\chi^2$, $\mathcal{H}_{-1} = \frac{1}{2}R\chi^2$, and $\mathcal{H}_{\frac{1}{2}} = 4\text{H}^2$.

B.2. Inequalities between f -Divergences

First, we show a general approach to obtain inequalities between f -divergences. Then, we prove the inequalities between squared Hellinger distance and Jensen-Shannon divergence. We also list the well-known Pinsker's inequality for completeness.

Lemma 16. Consider two f -divergences D_{f_1} and D_{f_2} with generator functions $f_1(\cdot)$ and $f_2(\cdot)$. If there exist two positive constants $0 < A < B$, such that for any $t \in [0, \infty)$, it holds that,

$$Af_2(t) \leq f_1(t) \leq Bf_2(t)$$

Then, for any two densities P and Q (such that $P \ll Q$), we have,

$$AD_{f_2}(P, Q) \leq D_{f_1}(P, Q) \leq BD_{f_2}(P, Q)$$

Proof. Note that we extend the domain of f_1 and f_2 by defining $f_1(0) = \lim_{t \downarrow 0} f_1(t)$ (and similar for f_2). We require $P \ll Q$ so that f -divergences are well-defined. In this sense, for any $x \in \Omega$, $P(x)/Q(x) \in [0, \infty)$ is defined, and we have $Af_2(P(x)/Q(x)) \leq f_1(P(x)/Q(x)) \leq Bf_2(P(x)/Q(x))$. Multiply non-negative $Q(x)$ and integrate over Ω . We obtain the desired inequality: $AD_{f_2}(P, Q) \leq D_{f_1}(P, Q) \leq BD_{f_2}(P, Q)$. \square

Theorem 17 (Theorem 11 of (Sason & Verdu, 2016)). For any two densities P and Q , (assume natural logarithm is used in the definition of Jensen-Shannon divergence), we have

$$(\ln 2)\text{H}^2(P, Q) \leq \text{JS}(P, Q) \leq \text{H}^2(P, Q)$$

Proof. Given Lemma 16, we only need to prove that for any $t \in [0, \infty)$, the following inequality holds,

$$(\ln 2)f_{\text{H}^2}(t) \leq f_{\text{JS}}(t) \leq f_{\text{H}^2}(t)$$

where the definitions of f_{H^2} and f_{JS} can be found in Table 4.

Note that when $t = 1$, all terms are 0 and the inequalities hold trivially. For $t \neq 1$, as $f_{H^2}(t) > 0$, we define,

$$\xi(t) = \frac{f_{JS}(t)}{f_{H^2}(t)} = \frac{t \ln \frac{2t}{t+1} + \ln \frac{2}{t+1}}{(\sqrt{t} - 1)^2}$$

$\xi(t)$ is defined on $[0, 1) \cup (1, \infty)$, We want to prove that $\ln 2 \leq \xi(t) \leq 1$ always holds. Its derivative is,

$$\xi'(t) = \frac{\sqrt{t} \ln \frac{2t}{t+1} + \ln \frac{2}{t+1}}{\sqrt{t} (1 - \sqrt{t})^3}$$

Denote the numerator above by $\xi_{(1)}(t)$. Its derivative is,

$$\xi'_{(1)}(t) = \frac{(t+1) \ln \frac{2t}{t+1} + 2(1 - \sqrt{t})}{2\sqrt{t}(t+1)}$$

Again, denote the numerator above by $\xi_{(2)}(t)$. Its derivative is,

$$\xi'_{(2)}(t) = \frac{1}{t} - \frac{1}{\sqrt{t}} + \ln \frac{2t}{t+1}$$

Using the well-known logarithm inequality: for any $x > 0$, $\ln x > 1 - \frac{1}{x}$, we have,

$$\xi'_{(2)}(t) \geq \frac{1}{t} - \frac{1}{\sqrt{t}} + 1 - \frac{t+1}{2t} = \frac{(\sqrt{t} - 1)^2}{2t} \geq 0$$

Also, since $\xi_{(2)}(1) = 0$, and the denominator of $\xi'_{(1)}(t)$ is always positive, hence,

$$\xi'_{(1)}(t) \begin{cases} < 0 & t \in [0, 1) \\ > 0 & t \in (1, \infty) \end{cases}$$

Because $\xi_{(1)}(1) = 0$, this implies $\xi_{(1)}(t) \geq 0$. Thus,

$$\xi'(t) \begin{cases} > 0 & t \in [0, 1) \\ < 0 & t \in (1, \infty) \end{cases}$$

That is, $\xi(t)$ is strictly increasing on $[0, 1)$, and is strictly decreasing on $(1, \infty)$. To determine its range, we only need to compute these limits: $\lim_{t \downarrow 0} \xi(t)$, $\lim_{t \uparrow 1} \xi(t)$, $\lim_{t \downarrow 1} \xi(t)$, and $\lim_{t \rightarrow +\infty} \xi(t)$:

$$\lim_{t \downarrow 0} \xi(t) = \ln 2$$

$$\lim_{t \uparrow 1} \xi(t) = \lim_{t \downarrow 1} \xi(t) = \lim_{t \rightarrow 1} \frac{\sqrt{t} \ln \frac{2t}{t+1}}{\sqrt{t} - 1} = \lim_{t \rightarrow 1} \frac{2\sqrt{t}^3}{t+1} = 1$$

$$\lim_{t \rightarrow +\infty} \xi(t) = \lim_{t \rightarrow +\infty} \frac{t \ln \frac{2t}{t+1}}{(\sqrt{t} - 1)^2} = \lim_{t \rightarrow +\infty} \frac{\ln \frac{2t}{t+1} + \frac{1}{t+1}}{\frac{\sqrt{t}-1}{\sqrt{t}}} = \ln 2$$

Together with the monotonic properties of $\xi(t)$, we know

$$\ln 2 \leq \xi(t) \leq 1$$

□

Theorem 18 (Pinsker's Inequality, Eq. (1) of (Sason & Verdu, 2016)). *For any two densities P and Q , we have,*

$$\text{TV}(P, Q) \leq \sqrt{\frac{1}{2} \text{KL}(P, Q)}$$

It is a well-known result. See for example Theorem 2.16 of (Massart, 2007) for a proof.

C. Wasserstein Distances: Formulas and Inequalities

C.1. Formulas for Wasserstein Distances

We list the algorithm and the formula to calculate the Wasserstein distance when space Ω is finite or the distributions P and Q are Gaussians.

Theorem 19. *For any two discrete distributions P, Q on a finite space $\Omega = \{\mathbf{x}_1, \dots, \mathbf{x}_n\}$, the p -Wasserstein distance W_p can be computed by the following linear program:*

$$\begin{aligned} W_p(P, Q)^p = & \min \sum_{i=1}^n \sum_{j=1}^n d^p(\mathbf{x}_i, \mathbf{x}_j) \pi_{ij} \\ \text{subject to } & \sum_{j=1}^n \pi_{ij} = P(\mathbf{x}_i) & i = 1, \dots, n \\ & \sum_{i=1}^n \pi_{ij} = Q(\mathbf{x}_j) & j = 1, \dots, n \\ & \text{and } \pi_{ij} > 0 & i = 1, \dots, n \text{ and } j = 1, \dots, n \end{aligned}$$

Useful discussions can be found in (Oberman & Ruan, 2015).

Theorem 20. *For any two non-degenerate Gaussians $P = \mathcal{N}(m_1, C_1)$ and $Q = \mathcal{N}(m_2, C_2)$ on \mathbb{R}^n , with respective means $m_1, m_2 \in \mathbb{R}^n$ and (symmetric positive semi-definite) covariance matrices $C_1, C_2 \in \mathbb{R}^{n \times n}$. The square of 2-Wasserstein distance W_2 between P, Q is,*

$$W_2(P, Q)^2 = \|m_1 - m_2\|_2^2 + \text{Tr} \left(C_1 + C_2 - 2 \left(C_1^{1/2} C_1 C_2^{1/2} \right)^{1/2} \right)$$

where $\|\cdot\|_2$ is the Euclidean norm.

See (Olkin & Pukelsheim, 1982) for a proof.

C.2. Inequalities between Wasserstein Distances and Total Variation Distance

Both Wasserstein distances and Total Variation distance can be regarded as optimal transportation costs. More specifically,

$$\begin{aligned} W_p(P, Q) &:= \left(\inf_{\gamma \in \Gamma(P, Q)} \int_{\Omega \times \Omega} d(x, y)^p d\gamma(x, y) \right)^{\frac{1}{p}} \\ \text{TV}(P, Q) &:= \inf_{\gamma \in \Gamma(P, Q)} \int_{\Omega \times \Omega} \mathbf{1}_{x \neq y} d\gamma(x, y) \end{aligned}$$

where $\Gamma(P, Q)$ denotes the set of all measures on $\Omega \times \Omega$ with marginals P and Q on variable x and y respectively, (also called the set of all possible couplings of P and Q). Bounding the distance $d(x, y)$ directly leads to inequalities between p -Wasserstein distance and Total Variation distance.

Theorem 21. *For any two distributions P and Q on a space Ω , if Ω is bounded with diameter $\text{diam}(\Omega) = \max\{d(x, y) | x, y \in \Omega\}$, then,*

$$W_p(P, Q)^p \leq \text{diam}(\Omega)^p \text{TV}(P, Q)$$

Moreover, if Ω is finite, let $d_{\min} = \min_{x \neq y} d(x, y)$ be the minimum mutual distance between pairs of distinct points in Ω , then,

$$W_p(P, Q)^p \geq d_{\min}^p \text{TV}(P, Q)$$

Proof. This theorem is a generalization of Theorem 4 of (Gibbs & Su, 2002). Since $d(\cdot, \cdot)$ is a metric of space Ω , $d(x, y) = 0$ if and only if $x = y$. Thus $d(x, y) \equiv d(x, y) \mathbf{1}_{x \neq y}$, and we have,

$$W_p(P, Q)^p = \inf_{\gamma \in \Gamma(P, Q)} \int_{\Omega \times \Omega} d(x, y)^p \mathbf{1}_{x \neq y} d\gamma(x, y)$$

If Ω is bounded, then for any x, y in Ω , it holds that $d(x, y) \leq \text{diam}(\Omega)$. Applying this inequality to the formula above leads to $W_p(P, Q)^p \leq \text{diam}(\Omega)^p \text{TV}(P, Q)$.

Similarly, if Ω is finite, then for any distinct $x \neq y$ in Ω , it holds that $d(x, y) \geq d_{\min}$. We can generalize it to: for any x, y in Ω , we have $d(x, y) \mathbf{1}_{x \neq y} \geq d_{\min} \mathbf{1}_{x \neq y}$. Applying this inequality to the formula above leads to $W_p(P, Q)^p \geq d_{\min}^p \text{TV}(P, Q)$. \square

D. Subadditivity Upper-Bounds at Different Levels-of-Detail

The subadditivity upper-bound $\sum_{i=1}^n \delta(P_{X_i \cup X_{\Pi_i}}, Q_{X_i \cup X_{\Pi_i}})$ depends on the structure of the Bayes-net. More specifically, the underlying DAG G determines the set of local neighborhoods $\{\{1\} \cup \Pi_1, \dots, \{n\} \cup \Pi_n\}$, and consequently, determines how we construct the set of discriminators of subadditive GANs. In this section, we discuss that the set of local neighborhoods in the subadditive bound can change either by truncating the induction process when deriving the subadditivity upper-bound (see the proof of Theorem 1 in Appendix A.1 for reference), or by contracting the neighboring nodes of the Bayes-net. Both methods result in a tighter subadditivity upper-bound at a coarser level-of-detail (i.e., with larger local neighborhoods). For the sake of simplicity, we limit the scope to Bayes-nets describing auto-regressive time series. For such graph G , there are T nodes $(\{1, \dots, T\})$, and each node depends on its p previous nodes; see Fig. 4a for an example.

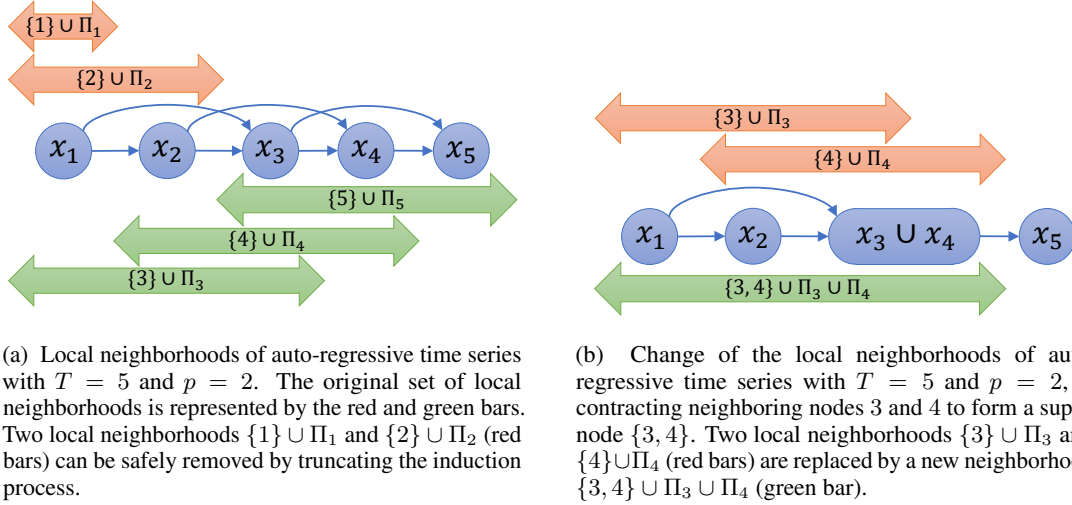


Figure 4. Changes of the local neighborhoods of a Bayes-net representing auto-regressive time series with $T = 5$ and $p = 2$, if we (a) truncate the induction process, or (b) contract a pair of neighboring nodes. In each case, the subadditivity upper-bound becomes tighter and characterize the Bayes-net at a coarser level-of-detail.

D.1. Truncation of Induction

For a probability divergence δ which satisfies subadditivity on Bayes-nets, the subadditivity upper-bound $\sum_{t=1}^T \delta(P_{X_t \cup X_{\Pi_t}}, Q_{X_t \cup X_{\Pi_t}})$ of $\delta(P, Q)$ is obtained by repeatedly applying the subadditivity of δ on Markov Chains of super-nodes $X_{\{1, \dots, s\} \setminus \Pi_{s+1}} \rightarrow X_{\Pi_{s+1}} \rightarrow X_{s+1}$, for $s = T - 1, T - 2, \dots, 1$. We can truncate the induction process and get an alternative upper-bound: $\delta(P, Q) < \delta(P_{\cup_{t=1}^s X_t}, Q_{\cup_{t=1}^s X_t}) + \sum_{t=s+1}^T \delta(P_{X_t \cup X_{\Pi_t}}, Q_{X_t \cup X_{\Pi_t}})$. This new upper-bound is tighter, but it does not encode the conditional independence information of the sub-sequence (X_1, \dots, X_s) . However, this alternative upper-bound is preferable if we choose s to be the largest number where its set of parents is exactly its previous nodes, i.e. $\Pi_s = \{1, \dots, s - 1\}$. The subadditivity inequality that we combined at induction step s is $\delta(P_{\cup_{t=1}^s X_t}, Q_{\cup_{t=1}^s X_t}) \equiv \delta(P_{X_{\Pi_s} \cup X_s}, Q_{X_{\Pi_s} \cup X_s}) \leq \delta(P_{\cup_{t=1}^{s-1} X_t}, Q_{\cup_{t=1}^{s-1} X_t}) + \delta(P_{X_{\Pi_s} \cup X_s}, Q_{X_{\Pi_s} \cup X_s})$ (corresponding to the second case in the proof of Theorem 1 in Appendix A.1). Truncating at such s avoids introducing the redundant term $\delta(P_{\cup_{t=1}^{s-1} X_t}, Q_{\cup_{t=1}^{s-1} X_t})$ into the upper-bound. As shown in Fig. 4a, for this specific example $s = p + 1 = 3$ is the largest number such that $\Pi_3 = \{1, 2\}$. Truncating at $s = 3$ removes $\{1\} \cup \Pi_1$ and $\{2\} \cup \Pi_2$ from the set of local neighborhoods, resulting in a more efficient subadditivity upper-bound $\sum_{t=3}^5 \delta(P_{X_t \cup X_{\Pi_t}}, Q_{X_t \cup X_{\Pi_t}})$. This is helpful for time series data, since it makes all local neighborhoods have the same number of dimensions. If all $X_t \in \mathbb{R}^d$, then for $t = 3, 4$ and 5 , $X_t \cup X_{\Pi_t} \in \mathbb{R}^{3d}$. In this sense, we can share a similar architecture among all the local discriminators in a subadditive GAN.

D.2. Neighboring Nodes Contraction

The set of local neighborhoods is determined by the structure G of the Bayes-net. Network contraction not only simplifies the Bayes-net but also leads to a tighter subadditivity upper-bound at a lower level-of-detail. Here, we only consider the contraction of neighboring nodes in a time series (X_1, \dots, X_T) . If we merge node s with $s + 1$ ($s = 1, \dots, T - 1$), and

form a super-node $\{s, s + 1\}$, local neighborhoods $\{s\} \cup \Pi_s$ and $\{s + 1\} \cup \Pi_{s+1}$ are replaced by $\{s, s + 1\} \cup \Pi_s \cup \Pi_{s+1}$, and the total number of neighborhoods decreases by one. As shown in Fig. 4b, when nodes 3 and 4 are merged, local neighborhoods $\{3\} \cup \Pi_3$ and $\{4\} \cup \Pi_4$ are replaced by $\{3, 4\} \cup \Pi_3 \cup \Pi_4$. We omit the conditional dependence between nodes 3 and 4, but reduce one discriminator in the subadditive GAN. Neighboring nodes contraction allows us to control the level-of-detail that the subadditivity upper-bound encodes flexibly. This can be useful when the variables in the Bayes-net have non-uniform dimensionalities.

E. Subadditivity on Markov Random Fields

In this section, we first review the 3-dimensional Gaussian counter-examples of the subadditivity of 2-Wasserstein distance. More specifically, we show that although Markov Random Field is the most appropriate probability graphical model to describe such Gaussians, they are also valid Bayes-nets, and thus can serve as counter-examples of subadditivity on Bayes-nets. Then, we move on to discuss how to obtain subadditivity upper-bounds on generic graphical models, using the same approach as in the proof of Theorem 1 in Appendix A.1. Using breadth-first search (BFS), we obtain a class of subadditivity upper-bounds on Markov Random Fields. Finally, we consider a particular type of Markov Random Fields: sequences with local dependencies but no natural directionality, e.g., sequences of words, and report a possible design of subadditive GANs on such sequences.

E.1. 3-Dimensional Gaussians with Markov Property

We consider non-degenerate 3-dimensional Gaussians with zero means $P = \mathcal{N}(\mathbf{0}, C)$ on variables (X, Y, Z) , which are also Bayes-nets with structure $X \rightarrow Y \rightarrow Z$. From the definition of Bayes-nets: each variable is conditionally independent of its non-descendants given its parent variables, we know P is a Bayes-net if and only if for any $x, y, z \in \mathbb{R}$, it holds that $P_{Z|X,Y}(z|x, y) = P_{Z|Y}(z|y)$. Let C_{ij} denote the element at the i -th row and j -th column of $C \in \mathbb{R}^{3 \times 3}$. It is not hard to compute that,

$$P_{Z|Y}(z|y) = \mathcal{N}\left(\frac{C_{32}}{C_{22}}y, C_{33} - \frac{C_{32}C_{23}}{C_{22}}\right)$$

$$P_{Z|X,Y}(z|x, y) = \mathcal{N}\left([C_{31} \quad C_{32}] \begin{bmatrix} C_{11} & C_{12} \\ C_{21} & C_{22} \end{bmatrix}^{-1} \begin{bmatrix} x \\ y \end{bmatrix}, C_{33} - [C_{31} \quad C_{32}] \begin{bmatrix} C_{11} & C_{12} \\ C_{21} & C_{22} \end{bmatrix}^{-1} \begin{bmatrix} C_{13} \\ C_{23} \end{bmatrix}\right)$$

Matching the means and variances of these two 1-dimensional Gaussians of z , we know that the two conditional distributions coincide if and only if $C_{32}C_{21} = C_{31}C_{22}$, i.e. the 2×2 upper-right (or equivalently, the lower-left) sub-matrix of C has zero determinant. It is clear that this requirement on the covariance matrix C is symmetric under switching variables X and Z . This means $P_{X|Y,Z}(x|y, z) = P_{X|Y}(x|y)$ holds simultaneously, and the most appropriate graphical model to describe such Gaussians is the Markov Random Field. However, as long as the Markov property $P_{Z|X,Y}(z|x, y) = P_{Z|Y}(z|y)$ holds, P is a valid Bayes-net, and the Counter-Example 1 we constructed is valid. These 3-dimensional Gaussians are special, as they satisfy the definitions of both Bayes-nets and Markov Random Fields.

E.2. Subadditivity on Markov Random Fields

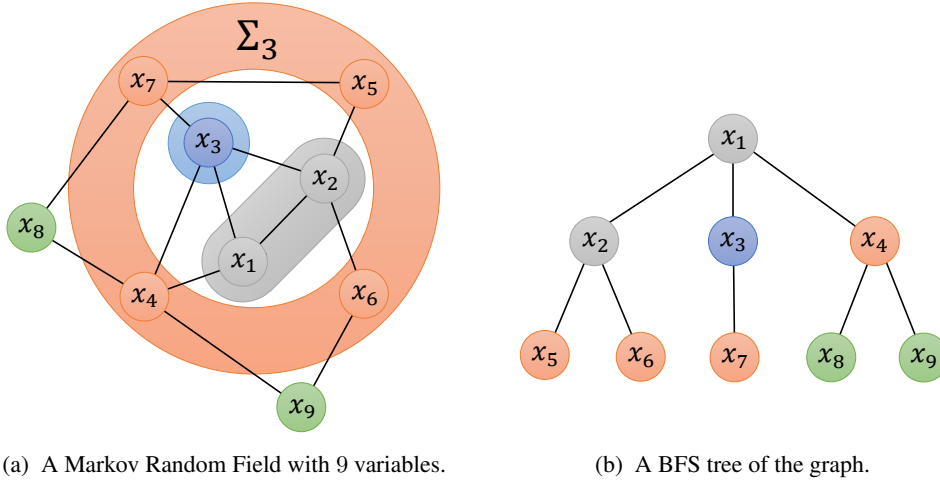
From the proof of Theorem 1 in Appendix A.1, we obtain the subadditivity upper-bound on Bayes-nets by repeatedly applying the subadditivity inequality on Markov Chain $X \rightarrow Y \rightarrow Z$. Moreover, we allow $X = \emptyset$ or $Y = \emptyset$ (i.e., X and Z are conditional independent), as addressed by the second and third cases in the proof. In general, for a generic probability graphical model with an underlying graph G (there may be directed and undirected edges in G), let P and Q be two distributions characterized by such graphical model. If δ satisfy subadditivity on Markov Chain $X \rightarrow Y \rightarrow Z$ with conditionally independent variables X and Y , we can obtain a subadditivity upper-bound on $\delta(P, Q)$ by the following procedure:

1. Choose an ordering of nodes $(1, \dots, n)$. The ordering is valid if the induction can be proceeded from start to end.
2. For node $k = 1, \dots, n - 1$, let Σ_k be the smallest set of nodes such that $\Sigma_k \subsetneq \{k + 1, \dots, n\}$ and X_k is conditionally independent of $\cup_{i=k+1}^n X_i$ given X_{Σ_k} , which can be written as $X_k \perp\!\!\!\perp \cup_{i=k+1}^n X_i \mid X_{\Sigma_k}$. If we cannot find such Σ_k , the ordering $(1, \dots, n)$ is invalid and the induction cannot be proceeded. Applying the subadditivity of δ on the Markov Chain of super-nodes $X_{\{k+1, \dots, n\} \setminus \Sigma_k} \rightarrow X_{\Sigma_k} \rightarrow X_k$ gives an inequality $\delta(P_{\cup_{i=k+1}^n X_i}, Q_{\cup_{i=k+1}^n X_i}) \leq \delta(P_{\cup_{i=k+1}^n X_i}, Q_{\cup_{i=k+1}^n X_i}) + \delta(P_{X_{\Sigma_k} \cup X_k}, Q_{X_{\Sigma_k} \cup X_k})$.

3. By combining all the inequalities obtained, we get a subadditivity upper-bound $\sum_{i=1}^n \delta(P_{X_{\Sigma_i} \cup X_i}, Q_{X_{\Sigma_i} \cup X_i}) \geq \delta(P, Q)$.

This process is identical to the proof of Theorem 1 for Bayes-nets, except that (1) we have to manually choose a valid ordering of nodes, and (2) the set of parents Π_k is replaced by the smallest set of nodes $X_{\Sigma_k} \subseteq \{k+1, \dots, n\}$ such that $X_k \perp\!\!\!\perp \cup_{i=k+1}^n X_i \mid X_{\Sigma_k}$, which depends on the ordering we choose. For Bayes-nets, the ordering we use is the reversed topological ordering, and for each k , we have $\Sigma_k = \Pi_k$.

Let us now illustrate this process on Markov Random Fields, whose underlying probability structure is described by undirected graphs. An enumeration of the nodes of a graph G is said to be a BFS ordering if it is a possible output of the BFS algorithm on this graph. If we use a BFS ordering $(1, \dots, n)$, then it is not hard to prove that for any $k \in \{1, \dots, n\}$, we have $\Sigma_k = \cup_{i=1}^k N_i \setminus \{1, \dots, k\}$, where N_i is the set of nodes adjacent to node i (i.e. the set of nearest neighbors). As shown in Fig. 5, if we choose a BFS ordering, Σ_k is actually the smallest set of nodes that surround the current and processed nodes $\{1, \dots, k\}$. Σ_k is called a separating subset between $\{1, \dots, k\}$ and $\{k+1, \dots, n\} \setminus \Sigma_k$, as every path from a node in $\{1, \dots, k\}$ to a node in $\{k+1, \dots, n\} \setminus \Sigma_k$ passes through Σ_k . By the global Markov property of Markov random fields, we indeed have $X_k \perp\!\!\!\perp \cup_{i=k+1}^n X_i \mid X_{\Sigma_k}$.



(a) A Markov Random Field with 9 variables.

(b) A BFS tree of the graph.

Figure 5. A local neighborhood $\{3\} \cup \Sigma_3$ of a Markov Random Field with 9 variables, if we use a BFS ordering of nodes $(1, \dots, 9)$. Where (a) is the Markov Random Field and (b) is the corresponding BFS tree. It is a snapshot of the induction process at $k = 3$. Where the gray nodes have been processed, the blue node is the current focus, the orange nodes represent the set Σ_3 , which is the smallest set such that $X_3 \perp\!\!\!\perp \cup_{i=4}^9 X_i \mid X_{\Sigma_3}$, and the green nodes are the rest.

E.3. Subadditive GANs for Sequences of Words

Now we consider a type of data, e.g. sequences of words, that can be characterized by Markov Random Fields. If we assume the distribution of a word depends on both the pre- and post- context, and consider up to $(2p+1)$ -grams (i.e. consider the distribution of up to $2p+1$ consecutive words), the corresponding Markov Random Field is an undirected graph G , where each node i is connected to its p previous nodes and p subsequent nodes. Let $(1, \dots, n)$ be the natural ordering of these n words. Clearly, both $(1, \dots, n)$ and $(n, \dots, 1)$ are valid BFS orderings. Following the method in Appendix E.2, and if we truncate the induction at step $k = n - p$ (see Appendix D.1 for details), these two orderings result in an identical subadditivity upper bound $\sum_{k=1}^{n-p} \delta(P_{\cup_{i=k}^{k+p} X_i}, Q_{\cup_{i=k}^{k+p} X_i})$. Each local neighborhoods contains $p+1$ consecutive words. Equipped with this theoretical-justified subadditivity upper-bound, we can use a set of small discriminators in GANs, each on a sub-sequence of $p+1$ consecutive words. This leads to a possible design of subadditive GANs for sequences of words.

F. Prior Work on Bounding the IPMs

We list some of the prior work on bounding the Integral Probability Metrics (IPMs). All the concepts and theorems introduced here are used by the proof of the IPM subadditivity upper-bound (Theorem 8) in Appendix A.6.

F.1. Preliminaries and Notations

Firstly, we introduce some concepts that help us characterize the set of discriminators \mathcal{F} . Consider \mathcal{F} as a set of some functions $\phi : \Omega \rightarrow \mathbb{R}$, where $\Omega \subseteq \mathbb{R}^{nd}$. The Banach space of bounded continuous functions is denoted by $C_b(\Omega) := \{\phi : \Omega \rightarrow \mathbb{R} \mid \phi \text{ is continuous and } \|\phi\|_\infty < \infty\}$, where $\|\phi\|_\infty = \sup_{x \in X} |\phi(x)|$ is the uniform norm. The linear span of \mathcal{F} is defined as,

$$\text{span}\mathcal{F} := \left\{ \alpha_0 + \sum_{i=1}^n \alpha_i \phi_i \mid \alpha_i \in \mathbb{R}, \phi_i \in \mathcal{F}, n \in \mathbb{N} \right\}$$

For a function $g \in \text{span}\mathcal{F}$, we define the \mathcal{F} -variation norm $\|g\|_{\mathcal{F}}$ as the infimum of the L_1 norm of the expansion coefficients of g over \mathcal{F} , that is,

$$\|g\|_{\mathcal{F}} = \inf \left\{ \sum_{i=1}^n |\alpha_i| \mid g = \alpha_0 + \sum_{i=1}^n \alpha_i \phi_i, \forall \alpha_i \in \mathbb{R}, \phi_i \in \mathcal{F}, n \in \mathbb{N} \right\}$$

Let $\text{cl}(\text{span}\mathcal{F})$ be the closure of the linear span of \mathcal{F} . We say $g \in \text{cl}(\text{span}\mathcal{F})$ is approximated by \mathcal{F} with an error decay function $\varepsilon(r)$ for $r \geq 0$, if there exists a $\phi_r \in \text{span}\mathcal{F}$, such that $\|\phi_r\|_{\mathcal{F}} \leq r$ and $\|g - \phi_r\|_\infty \leq \varepsilon(r)$. In this sense, it is not hard to show that $g \in \text{cl}(\text{span}\mathcal{F})$ if and only if $\inf_{r \geq 0} \varepsilon(r) = 0$.

F.2. The Universal Approximation Theorems

From Theorem 2.2 of (Zhang et al., 2018), we know that $d_{\mathcal{F}}(P, Q)$ is discriminative, i.e. $d_{\mathcal{F}}(P, Q) = 0 \iff P = Q$, if and only if $C_b(X)$ is contained in the closure of $\text{span}\mathcal{F}$, i.e. $C_b(X) \subseteq \text{cl}(\text{span}\mathcal{F})$. In other words, it means that we require $\text{span}\mathcal{F}$ to be dense in $C_b(X)$, so that $d_{\mathcal{F}}(P, Q) \rightarrow 0$ implies the weak converge of the fake distribution Q to the real distribution P .

By the famous universal approximator theorem (e.g. Theorem 1 of (Leshno et al., 1993)), the discriminative criteria $C_b(X) \subseteq \text{cl}(\text{span}\mathcal{F})$ can be satisfied by small discriminator sets such as the neural networks with only a single neuron, $\mathcal{F} = \{\sigma(w^T x + b) \mid w \in \mathbb{R}^{nd}, b \in \mathbb{R}\}$, if the activation function $\sigma : \mathbb{R} \rightarrow \mathbb{R}$ is continuous but not a polynomial. Later, (Bach, 2017) proves that the set of single-neuron neural networks with rectified linear unit (ReLU) activation also satisfies the criteria.

Theorem 22 (Theorem 1 of (Leshno et al., 1993), (Bach, 2017)). *For the set of neural networks with a single neuron, i.e. $\mathcal{F} = \{\sigma(w^T x + b) \mid w \in \mathbb{R}^{nd}, b \in \mathbb{R}\}$. The linear span of \mathcal{F} is dense in the Banach space of bounded continuous functions $C_b(X)$, i.e. $C_b(X) \subseteq \text{cl}(\text{span}\mathcal{F})$, if the activation function $\sigma(\cdot)$ is continuous but not a polynomial, or if $\sigma(u) = \max\{u, 0\}^\alpha$ for some $\alpha \in \mathbb{N}$ (when $\alpha = 1$, $\sigma(u) = \max\{u, 0\}$ is the ReLU activation).*

See (Leshno et al., 1993) and (Bach, 2017) for further details and the proofs.

F.3. IPMs Upper-Bounding the Jeffrey Divergence

(Zhang et al., 2018) explains how IPMs can control the likelihood function, so that along with the training of an IPM-based GAN, the training likelihood should generally increase. More specifically, they prove that if the densities P and Q exist, and $\log(P/Q)$ is inside the closure of the linear span of \mathcal{F} , i.e. $\log(P/Q) \in \text{cl}(\text{span}\mathcal{F})$, a function of the IPM $d_{\mathcal{F}}(P, Q)$ can upper-bound the Jeffrey divergence $\text{JF}(P, Q)$. In this sense, minimizing the IPM leads to the minimization of Jeffrey divergence (and thus KL divergence), which is equivalent to the maximization of the training likelihood.

Theorem 23 (Proposition 2.7 and 2.9 of (Zhang et al., 2018)). *Any function g inside the closure of the linear span of \mathcal{F} , i.e. $g \in \text{cl}(\text{span}\mathcal{F})$, is approximated by \mathcal{F} with an error decay function $\varepsilon(r)$. It satisfies,*

$$\left| \mathbb{E}_{x \sim P}[g(x)] - \mathbb{E}_{x \sim Q}[g(x)] \right| \leq 2\varepsilon(r) + r d_{\mathcal{F}}(P, Q) \quad \forall r \geq 0$$

Moreover, consider two distributions with positive densities P and Q , if $g = \log(P/Q) \in \text{cl}(\text{span}\mathcal{F})$, we have,

$$\text{JF}(P, Q) \equiv \left| \mathbb{E}_{x \sim P}[\log(P(x)/Q(x))] - \mathbb{E}_{x \sim Q}[\log(P(x)/Q(x))] \right| \leq 2\varepsilon(r) + r d_{\mathcal{F}}(P, Q) \quad \forall r \geq 0$$

Proof. The proof is in Appendix C of (Zhang et al., 2018). We repeat the proof here for completeness.

Since g is approximated by \mathcal{F} with error decay function $\varepsilon(r)$, for any $r \geq 0$, there exist some $\phi_r \in \text{span}\mathcal{F}$, which can be represented as $\phi_r = \sum_{i=1}^n \alpha_i \phi_i + \alpha_0$ with some $\alpha_i \in \mathbb{R}$ and $\phi_i \in \mathcal{F}$, such that $\sum_{i=1}^n |\alpha_i| = \|\phi_r\|_{\mathcal{F}} \leq r$ and $\|g - \phi_r\|_{\infty} < \varepsilon(r)$. In this sense, we have,

$$\begin{aligned}
 & \left| \mathbb{E}_{x \sim P}[g(x)] - \mathbb{E}_{x \sim Q}[g(x)] \right| \\
 &= \left| (\mathbb{E}_{x \sim P}[g(x)] - \mathbb{E}_{x \sim P}[\phi_r(x)]) - (\mathbb{E}_{x \sim Q}[g(x)] - \mathbb{E}_{x \sim Q}[\phi_r(x)]) + (\mathbb{E}_{x \sim P}[\phi_r(x)] - \mathbb{E}_{x \sim Q}[\phi_r(x)]) \right| \\
 &\leq \left| \mathbb{E}_{x \sim P}[g(x) - \phi_r(x)] \right| + \left| \mathbb{E}_{x \sim Q}[g(x) - \phi_r(x)] \right| + \left| \mathbb{E}_{x \sim P}[\phi_r(x)] - \mathbb{E}_{x \sim Q}[\phi_r(x)] \right| \\
 &\leq \mathbb{E}_{x \sim P}|g(x) - \phi_r(x)| + \mathbb{E}_{x \sim Q}|g(x) - \phi_r(x)| + \left| \sum_{i=1}^n \alpha_i (\mathbb{E}_{x \sim P}[\phi_i(x)] - \mathbb{E}_{x \sim Q}[\phi_i(x)]) \right| \\
 &\leq 2\varepsilon(r) + \sum_{i=1}^n |\alpha_i| \left| \mathbb{E}_{x \sim P}[\phi_i(x)] - \mathbb{E}_{x \sim Q}[\phi_i(x)] \right| \\
 &\leq 2\varepsilon(r) + r d_{\mathcal{F}}(P, Q)
 \end{aligned}$$

Applying this inequality to $g = \log(P/Q)$ proves that, for any $r \geq 0$, this linear function of IPM $2\varepsilon(r) + r d_{\mathcal{F}}(P, Q)$ upper-bounds the Jeffrey divergence $\text{JF}(P, Q)$. \square

The upper-bounds obtained by Theorem 23 are a set linear functions of the IPM, $\{2\varepsilon(r) + r d_{\mathcal{F}}(P, Q) \mid r \geq 0\}$. In order to prove that the IPM $d_{\mathcal{F}}(P, Q)$ can upper-bound the Jeffrey divergence $\text{JF}(P, Q)$ up to some constant coefficient and additive error, i.e. $\alpha \text{JF}(P, Q) - \epsilon \leq d_{\mathcal{F}}(P, Q)$ for some constants $\alpha, \epsilon > 0$, we have to control both $\varepsilon(r)$ and r simultaneously. Because $\lim_{r \rightarrow \infty} \varepsilon(r) = 0$, all we need is an efficient upper-bound on $\varepsilon(r)$ for large enough r , which is provided in (Bach, 2017).

Theorem 24 (Proposition 6 of (Bach, 2017)). *For a bounded space Ω , let $g : \Omega \rightarrow \mathbb{R}$ be a bounded and Lipschitz continuous function (i.e. there exists a constant $\eta > 0$ such that $\|g\|_{\infty} < \eta$ and for any $x, y \in \Omega \subseteq \mathbb{R}^{nd}$, it holds that $\|g(x) - g(y)\|_{\infty} \leq \frac{1}{\text{diam}\Omega} \eta \|x - y\|_2$), and let \mathcal{F} be a set of neural networks with a single neuron, which have ReLU activation and bounded parameters (i.e. $\mathcal{F} = \{\max\{w^T x + b, 0\} \mid w \in \mathbb{R}^{nd}, b \in \mathbb{R}, \|[w, b]\|_2 = 1\}$). Then, we have $g \in \text{cl}(\text{span}\mathcal{F})$, and g is approximated by \mathcal{F} with error decay function $\varepsilon(r)$, such that,*

$$\varepsilon(r) \leq C(nd) \eta \left(\frac{r}{\eta} \right)^{-\frac{2}{nd+1}} \log \left(\frac{r}{\eta} \right) \quad \forall r \geq R(nd)$$

where $C(nd), R(nd)$ are constants which only depend on the number of dimensions, nd .

See Proposition 3, Appendix C.3, and Appendix D.4 of (Bach, 2017) for the proof.

G. Examples of Local Subadditivity

In this section, we discuss a notable class of f -divergences that satisfy local subadditivity, namely the α -divergences. α -Divergences are f -divergences whose generator functions $f_{\mathcal{H}_\alpha}(\cdot)$ generalize power functions (Table 4). We show that all α -divergences satisfy linear subadditivity when the distributions are two-sided close, and α -divergences with $\alpha > 0$ satisfy linear subadditivity when the distributions are only one-sided close.

Since for any $\alpha \in \mathbb{R}$, $f_{\mathcal{H}_\alpha}(t)$ is continuous with respect to t , and its second order derivative at $t = 1$, i.e. $f''_{\mathcal{H}_\alpha}(1) = t^{\alpha-2}|_{t=1} = 1$ is positive, by Theorem 10 we conclude the following result.

Example 2. α -divergences,

$$\mathcal{H}_\alpha(P, Q) := \begin{cases} \frac{1}{\alpha(\alpha-1)} \int Q((P/Q)^\alpha - 1) dx & \alpha \neq 0, 1 \\ \text{KL}(P, Q) & \alpha = 1 \\ \text{KL}(Q, P) & \alpha = 0 \end{cases}$$

which generalize KL and reverse KL divergences, χ^2 and reverse χ^2 divergences, and squared Hellinger distance (see Appendix B.1 for details), satisfy linear subadditivity when the two distributions P and Q are two-sided ϵ -close for some $\epsilon > 0$.

For α -divergences with $\alpha > 0$, apart from the above-mentioned properties, $f_{\mathcal{H}_\alpha}(t)$ is strictly convex since for any $t \in (0, \infty)$, we have $f''_{\mathcal{H}_\alpha}(t) = t^{\alpha-2} > 0$. And $f(0) = \lim_{t \downarrow 0} f(t)$ is always finite, because when $\alpha = 1$, we have $\lim_{t \downarrow 0} f(t) = 0$, and when $\alpha > 0$ and $\alpha \neq 1$, the limit $\lim_{t \downarrow 0} f(t) = -\frac{1}{\alpha(\alpha-1)}$ exists. By Theorem 11, we obtain the following.

Example 3. α -divergences with $\alpha > 0$, which generalize KL divergence, χ^2 divergence, and squared Hellinger distance, satisfy linear subadditivity when the two distributions P and Q are one-sided ϵ -close for some $\epsilon > 0$.

H. Miscellaneous Experiments

In this section, we report some more experimental results. Moreover, we discuss the advantages of our subadditive GAN framework compared with standard GANs using recurrent neural network (RNN) discriminators.

H.1. More Experimental Results

Diversity is one of the three aspects we considered when evaluating the generation quality of a GAN in Section 6. More specifically, we calculate the energy statistics between the real and fake samples, as a distance metric between the two distributions. However, a much more intuitive way to evaluate how closely the distribution of the generated samples resembles the real distribution is to visualize and compare their t-SNE (Maaten & Hinton, 2008) embeddings. Scatter plots of the t-SNE embeddings of the real and fake samples, when training on the five synthetic datasets as in Table 1, are shown in Fig. 6. We can see that on all the dataset, samples generated by subadditive GANs (the first row) resembles the real distribution better, compared with the standard GANs (the second row).

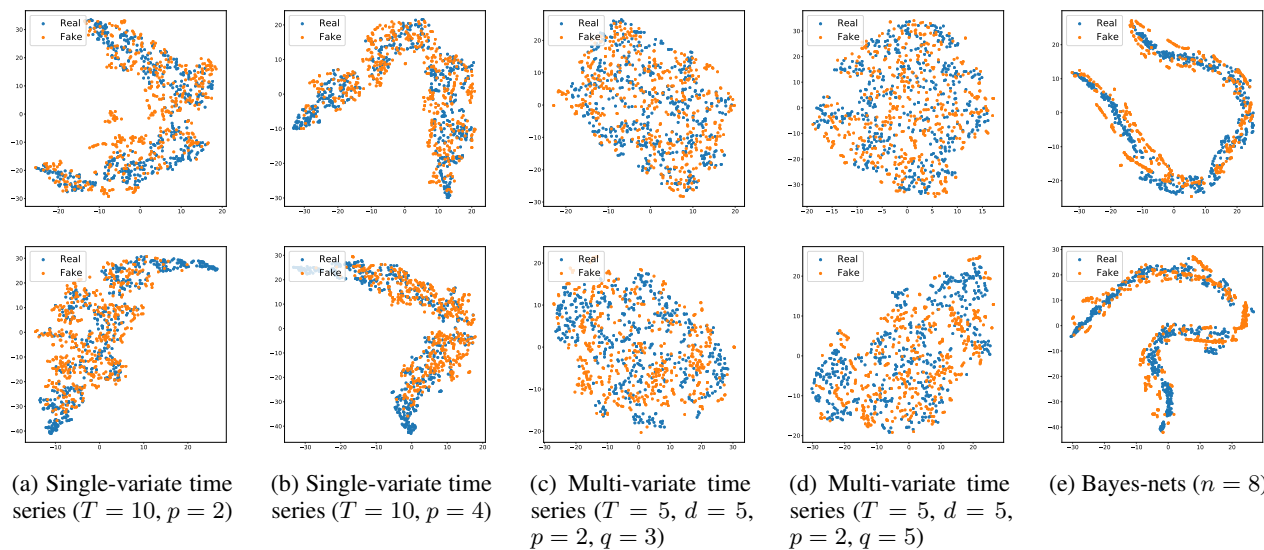


Figure 6. t-SNE visualization of the real and fake samples generated by subadditive GANs (first row) and standard GANs (second row) on (a) and (b): single-variate time series, (c) and (d): multi-variate time series, and (e): Bayes-nets.

H.2. Subadditive GANs vs. RNN Discriminators

Our subadditive GAN framework is suitable for time series with strong temporal correlations. However, recurrent neural networks (RNNs) are also capable of capturing the temporal dynamics of long time-series. Moreover, RNNs are efficient, as the number of parameters does not increase with the total length T of the sequence. In this regard, one may ask why we prefer subadditive GANs, instead of simply using RNN discriminators. We answer this question by summarizing the advantages of subadditive GANs, in comparison to RNN discriminators:

1. Unlike RNNs, Subadditive GANs explicitly encode the conditional independence information of the input time series into the objective. By exploiting such explicit dependency structure, Subadditive GANs are capable of decomposing the high-dimensional data into low-dimensional fragments in a natural way, greatly enhancing the training procedure.

2. Unlike RNNs, the objective of Subadditive GANs is a principled upper bound on the distance between the observed and generated distributions. Since discriminators of subadditive GANs are applied locally, the local distance approximation in subadditive upper bound is often tight as long as the set of discriminators are not too simple. This means that the discriminator loss of a subadditive GAN must be large if the real and fake distributions still differ significantly. The situation of RNN discriminators, however, is the opposite. Because RNN blocks use the same parameters, the IPM based on a set of RNNs can be significantly *lower* than the true distance. In this sense, the loss of an RNN discriminator can be very small while the true distance between observed and generated distributions is large.
3. In subadditive GANs, local discriminators can partially share their parameters to control the trade-off between their discriminative power and the training complexity. In contrast, the weights of RNN discriminator blocks are shared across the entire time series.

I. Experimental Setups

In this section, we list the setups of the experiments in Section 6 and Appendix H.

I.1. Synthetic Data-sets

We generate three types of synthetic Bayes-nets:

1. Single-Variate Time Series: Bayes-nets with T variables: $(X_1, \dots, X_T) \in \mathbb{R}^T$ and each $X_t \in \mathbb{R}$, defined by:

$$X_t = \sum_{i=1}^p \varphi_i X_{t-i} + \varepsilon_t \quad \forall t \in \{1, \dots, T\}$$

where $p \in \mathbb{N}$ and $0 < p < T$, the initial terms X_{-p+1}, \dots, X_0 are i.i.d. unit Gaussians (they are not a part of the generated data).

2. Multi-Variate Time Series: Bayes-nets with $T \times d$ variables: $\begin{pmatrix} X_{1,1} & \dots & X_{T,1} \\ \vdots & \vdots & \vdots \\ X_{1,d} & \dots & X_{T,d} \end{pmatrix} \in \mathbb{R}^{T \times d}$ and each $X_{t,k} \in \mathbb{R}$. Note

that although there are d features per time unit, different features are modeled as separated nodes in the Bayes-net. They are defined by:

$$X_{t,k} = \sum_{i=1}^p \sum_{j=-(q-1)/2}^{(q-1)/2} \varphi_i \psi_j X_{t-i, (k-j) \bmod d} + \varepsilon_{t,k} \quad \forall t \in \{1, \dots, T\}, \forall k \in \{1, \dots, d\}$$

where $q \in \mathbb{N}$ is a odd integer, and the initial terms $X_{-p+1,1}, \dots, X_{-p+1,d}, \dots, X_{0,1}, \dots, X_{0,d}$ are i.i.d. unit Gaussians (they are not a part of the generated data).

3. Bayes-Nets: Bayes-nets with n variables: $(X_1, \dots, X_n) \in \mathbb{R}^n$ and each $X_i \in \mathbb{R}$. Assume the underlying DAG is G , which determines the set of parents Π_i of each node i . They are defined by:

$$X_i = \sum_{j \in \Pi_i} \varphi_{j \rightarrow i} X_j + \varepsilon_i \quad \forall i \in \{1, \dots, n\}$$

where variables with no parents $\{X_i | \Pi_i = \emptyset\}$ are the initial terms and are i.i.d. unit Gaussians (they are a part of the generated data). We consider the DAG G as the Hasse diagram of all the $n = 2^k$ subsets of a k -element set $\{e_1, \dots, e_k\}$ ordered by inclusion. That is, the set of nodes is $V = \{S | S \subseteq \{e_1, \dots, e_k\}\}$ and there is a directed edge from node S_1 to S_2 if and only if $S_1 \subsetneq S_2$.

For all the three cases, the noise terms ε 's are i.i.d. 1-dimensional Gaussians with zero mean and standard deviation $\sigma = 0.1$.

I.2. Model Architectures

Subadditive GANs consist of a generator and a set of small discriminators. Different model architectures are used for different types of data:

1. Synthetic Single-Variate and Multi-Variate Time Series: Generator is a 3- or 4-layer Gated Recurrent Units (GRU) RNN. Discriminators are 2-layer GRU RNNs if the length of the local subsequence is larger than 4; otherwise, 1-dimensional CNNs are used.
2. Synthetic Bayes-Nets: Generator is a 6-layer Multi-Layer Perceptron (MLP). Discriminators are 3-layer MLPs.
3. Real-World Time Series: Generator is a 4-layer GRU RNN or a 6- to 11-layer 1-dimensional CNN. Discriminators are 3- or 4-layer GRU RNNs or 5- to 9-layer 1-dimensional CNNs.

I.3. Training Setups and Hyper-Parameters

For synthetic datasets, we train on a set of 2000 samples (training set) and evaluate against another set of 2000 samples (testing set). While for real-world datasets, we randomly choose 5000 samples from the pre-defined training and testing set. We train for 200 epochs on synthetic data, and 300~500 epochs on real-world time series. We always set the learning rate to 0.001. We use gradient penalty (WGAN-GP) (Gulrajani et al., 2017) to train Wasserstein GANs. The number of discriminator iterations per generator iteration is 5 for Wasserstein GANs and is 3 for other types of GANs. When comparing between subadditive and standard GANs, we use precisely the same set of training hyper-parameters.

The most critical hyper-parameter of subadditive GANs on real-world time series with unknown conditional independence structure is the hypothetical temporal correlation length p (i.e., the number of previous time units a variable depends on). We use grid-searches to find the best hypothetical correlation length. The physical nature of the dataset generally determines the range of the correlation length to consider. For example, for the basketball player trajectory dataset, we assume that the current movement of a player is affected by the positions of all the players within 2 seconds. Since the positions are recorded per $12/50 = 0.24$ seconds, the maximum hypothetical correlation length we need to consider is $2/0.24 \approx 8$.

For each experimental configuration, the experiment is repeated five times with newly generated synthetic data (if on synthetic datasets), or with different random partitions of the data (if on real-world datasets). The models are trained on an NVIDIA RTX 2080 Ti GPU with 11GB memory.

I.4. Evaluation Setups

Setups of the evaluation methods are listed as follows,

1. t-SNE Scatter Plots: We randomly select 500 testing samples and 500 generated samples and compute their t-SNE embeddings using standard libraries.
2. Energy Statistics: We compute the energy statistics between the testing set and generated set using standard libraries.
3. Discriminative Scores: We train a 1- or 2-layer GRU RNN classifier (for time series datasets) or a 3-layer MLP (for synthetic Bayes-nets) to distinguish between the testing and generated samples. We train for 50 epochs with a learning rate of 0.001. We report the training AUC (area under the ROC curve) as the discriminative score.
4. Predictive Scores: We train a 1- or 2-layer GRU RNN future predictor on the generated samples and test it on the testing samples. Note that this metric is designed for time series but not generic Bayes-nets. We report the testing MSE (mean-squared error) as the predictive score.

J. Verification of Subadditivity of Statistical Divergences

In this section, we verify the subadditivity of squared Hellinger distance, KL-divergence, Jeffrey divergence, and the generalized linear subadditivity of Jensen-Shannon divergence, Total Variation distance, 1-Wasserstein distance, and 2-Wasserstein distance on binary auto-regressive sequences in a finite space Ω .

To construct a simple Bayes-net P on a sequence of bits $(X_1, \dots, X_n) \in \{0, 1\}^n$, consider the auto-regressive sequence defined by,

$$P(X_t = 1 | X_{t-1}, \dots, X_{t-p}) = \sigma\left(\sum_{i=1}^p \varphi_i X_{t-i}\right)$$

where $p \in \mathbb{N}$ such that $0 < p < n$ is called the order of this auto-regressive sequence, and $[\varphi_1, \dots, \varphi_n]$ are the coefficients. The marginal distributions of the initial variables X_1, \dots, X_p have to be pre-defined. We assume they are conditionally independent, and define,

$$P(X_i = 1) = \psi_i \quad \forall i \in \{1, \dots, p\}$$

where for any $i \in \{1, \dots, p\}$, $\psi_i \in [0, 1]$. If the distribution of a binary sequence (X_1, \dots, X_n) follows the definitions above, we say it is a binary auto-regressive sequence of order p with coefficients $[\varphi_1, \dots, \varphi_n]$ and initials $[\psi_1, \dots, \psi_n]$.

Binary auto-regressive sequences are Bayes-nets, because each variable X_t is conditionally independent of its non-descendants given its parent variables X_{t-1}, \dots, X_{t-p} . The probabilistic graph G is determined by the length n and the order p . For a statistical divergence δ satisfying subadditivity, as described in Appendix D.1, we truncate the induction process and get a subadditivity upper-bound $\sum_{t=p+1}^n \delta(P_{\cup_{i=t-p}^t X_i}, Q_{\cup_{i=t-p}^t X_i})$. We verify that the subadditivity inequality (or linear subadditivity inequality) holds for various statistical divergences, on two specific examples.

Example 4 (Binary Auto-Regressive Sequences with Different Local Dependencies). *Consider binary auto-regressive sequences $(X_1, X_2, X_3, X_4) \in \{0, 1\}^4$ of order $p = 2$ with initials $[\psi_1, \psi_2] = [\frac{1}{2}, \frac{1}{2}]$. Two distributions P^x (with coefficients $[\varphi_1, \varphi_2] = [0, x]$) and Q^y (with coefficients $[\varphi_1, \varphi_2] = [0, y]$) are Bayes-nets with identical underlying structure. Divergence $\delta(P^x, Q^y)$ is a function of the parameters (x, y) . For all $(x, y) \in \{(x, y) \in \mathbb{R}^2 | x \neq y\}$, we have $\delta(P^x, Q^y) < \sum_{t=p+1}^n \delta(P_{\cup_{i=t-p}^t X_i}^x, Q_{\cup_{i=t-p}^t X_i}^y)$ if δ satisfies subadditivity, or $\alpha \cdot \delta(P^x, Q^y) < \sum_{t=p+1}^n \delta(P_{\cup_{i=t-p}^t X_i}^x, Q_{\cup_{i=t-p}^t X_i}^y)$ if δ satisfies α -linear subadditivity.*

Example 5 (Binary Auto-Regressive Sequences with Different Initial Distributions). *Consider binary auto-regressive sequences $(X_1, X_2, X_3, X_4) \in \{0, 1\}^4$ of order $p = 2$ with coefficients $[\varphi_1, \varphi_2] = [1, -1]$. Two distributions P^x (with initials $[\psi_1, \psi_2] = [\frac{1}{2}, x]$) and Q^y (with initials $[\psi_1, \psi_2] = [\frac{1}{2}, y]$) are Bayes-nets with identical underlying structure. Divergence $\delta(P^x, Q^y)$ is a function of the parameters (x, y) . For all $(x, y) \in \{(x, y) \in \mathbb{R}^2 | 0 < x \neq y < 1\}$, we have $\delta(P^x, Q^y) < \sum_{t=p+1}^n \delta(P_{\cup_{i=t-p}^t X_i}^x, Q_{\cup_{i=t-p}^t X_i}^y)$ if δ satisfies subadditivity, or $\alpha \cdot \delta(P^x, Q^y) < \sum_{t=p+1}^n \delta(P_{\cup_{i=t-p}^t X_i}^x, Q_{\cup_{i=t-p}^t X_i}^y)$ if δ satisfies α -linear subadditivity.*

We verify the subadditivity of H^2 , KL, JF, and the linear subadditivity of JS, TV, W_1 and W_2 on these two examples, as shown in Fig. 7. We draw contour plots of the subadditivity gap $\Delta = \sum_{t=p+1}^n \delta(P_{\cup_{i=t-p}^t X_i}^x, Q_{\cup_{i=t-p}^t X_i}^y) - \delta(P^x, Q^y)$ (if δ satisfies subadditivity) or $\Delta = \sum_{t=p+1}^n \delta(P_{\cup_{i=t-p}^t X_i}^x, Q_{\cup_{i=t-p}^t X_i}^y) - \alpha \cdot \delta(P^x, Q^y)$ (if δ satisfies α -linear subadditivity). All the inequalities are verified as we can visually confirm all contours are positive.

K. Verification of Local Approximations of f -Divergences

In this section, we observe the local behavior of common f -divergences when the two distributions P and Q are sufficiently close. And we verify the conclusion of Lemma 14: all f -divergences D_f with a generator function $f(t)$ that is twice differentiable at $t = 1$ and satisfies $f''(1) > 0$ have similar local approximations up to a constant factor up to $\mathcal{O}(\epsilon^3)$. More specifically, for a pair of two-sided ϵ -close distributions P and Q , we verify all such f -divergences satisfy:

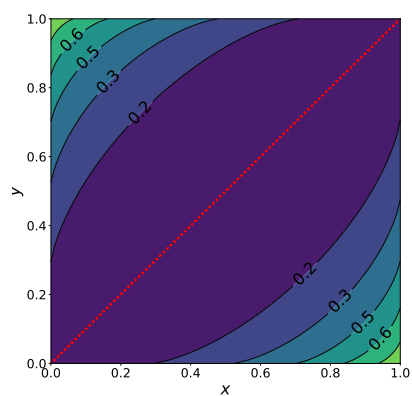
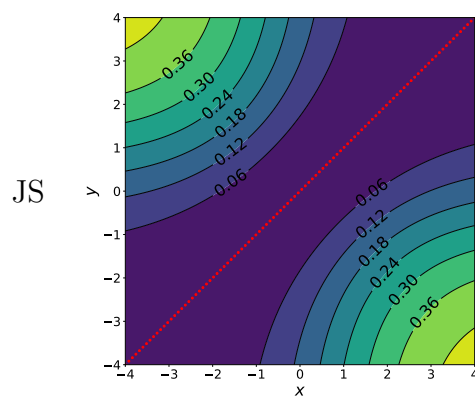
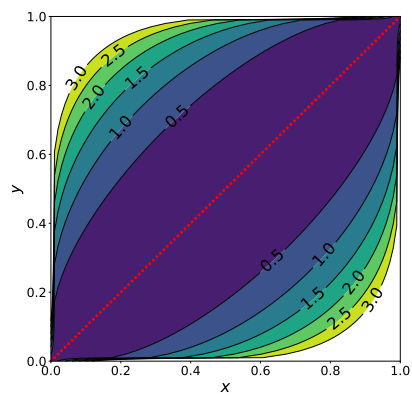
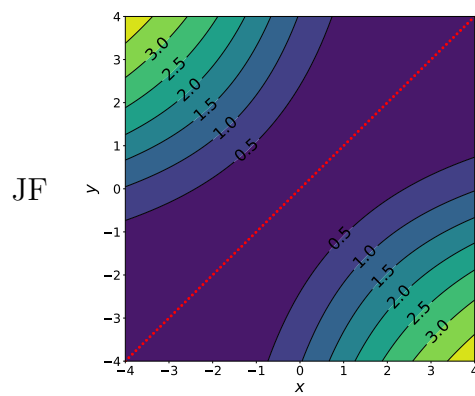
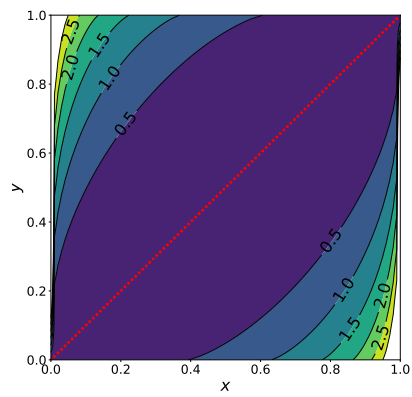
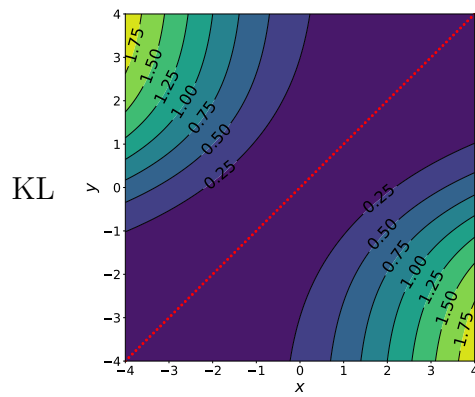
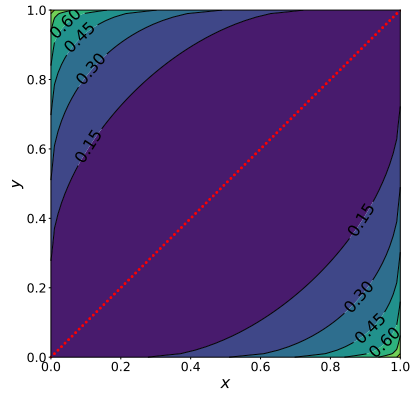
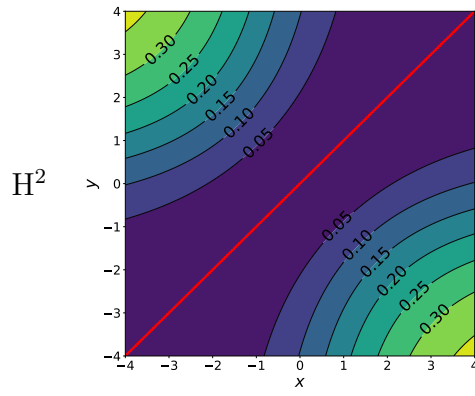
$$D_f(P, Q) = \frac{f''(1)}{2} \chi^2(P, Q) + \mathcal{O}(\epsilon^3)$$

Let us consider a simple example of two-sided close distributions on $\Omega = \mathbb{R}$. Suppose $Q = \mathcal{N}(0, 1)$ is the 1-dimensional unit Gaussian. Let $P(x) = (1 + \epsilon \sin(x))Q(x)$ for some $\epsilon \in (0, 1)$. It is easy to verify that P is a valid probability distribution: $\int_{-\infty}^{\infty} P(x)dx = \int_{-\infty}^{\infty} Q(x)dx + \epsilon \int_{-\infty}^{\infty} \sin(x)Q(x)dx = 1$, where the term $\int_{-\infty}^{\infty} \sin(x)Q(x)dx$ vanishes because $Q(x)$ is an even function and $\sin(x)$ is odd. Since for any $x \in \Omega = \mathbb{R}$, it holds that $P(x)/Q(x) = 1 + \epsilon \sin(x) \in [1 - \epsilon, 1 + \epsilon]$, we know P and Q are two-sided ϵ -close.

We compute several common f -divergences between such P and Q , for different $\epsilon \in [0, 0.5]$, as shown in Fig. 8a. We can see that, except for Total Variation distance which has a generator f_{TV} not differentiable at 1, all common f -divergences behave similarly up to a constant factor. Actually, these curves cluster into three groups according to $f''(1)$. In the first

Example 4

Example 5



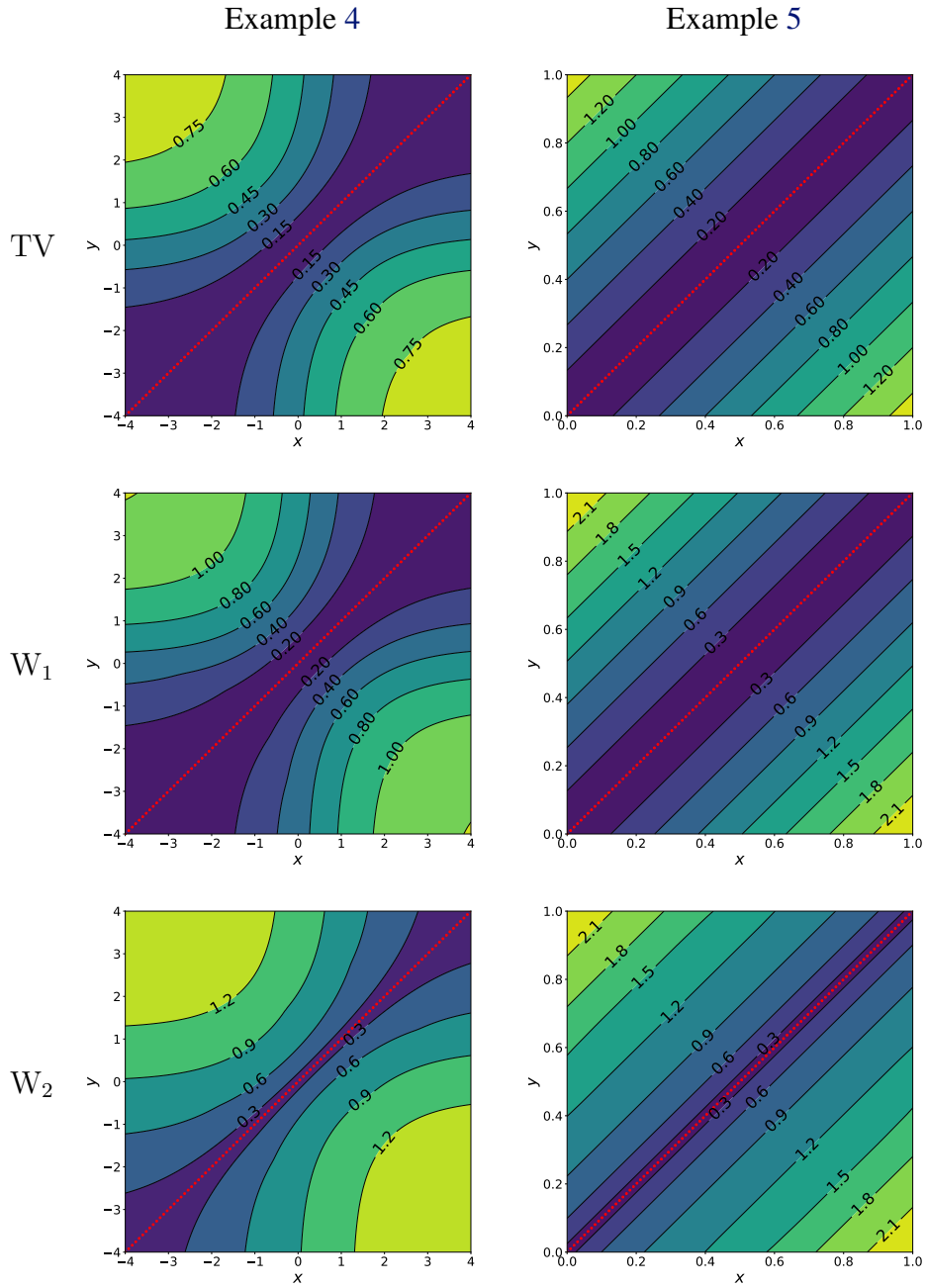
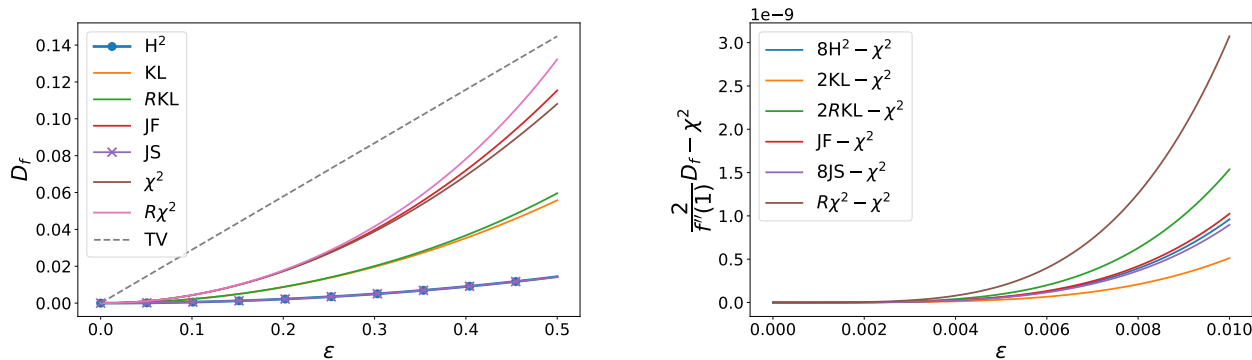


Figure 7. Contour maps showing the binary auto-regressive sequence examples of subadditivity or linear subadditivity of H^2 , KL, JF, JS, TV, W_1 , and W_2 . The two distributions P^x, Q^y are distributions of binary auto-regressive sequences with length $n = 4$ and order $p = 2$, following definitions in Example 4 and Example 5. The contours and colors indicate the subadditivity gap $\Delta = \sum_{t=p+1}^n \delta(P_{\cup_{i=t-p}^t X_i}^x, Q_{\cup_{i=t-p}^t X_i}^y) - \delta(P^x, Q^y)$ (if δ satisfies subadditivity) or $\Delta = \sum_{t=p+1}^n \delta(P_{\cup_{i=t-p}^t X_i}^x, Q_{\cup_{i=t-p}^t X_i}^y) - \alpha \cdot \delta(P^x, Q^y)$ (if δ satisfies α -linear subadditivity). The red line indicate places where the subadditivity gap is 0. White regions have too large subadditivity gap to be colored.

cluster: $f''_{\text{JF}}(1) = f''_{\chi^2}(1) = f''_{R\chi^2}(1) = 2$. In the second cluster: $f''_{\text{KL}}(1) = f''_{R\text{KL}}(1) = 1$. While in the third cluster: $f''_{\text{H}^2}(1) = f''_{\text{JS}}(1) = \frac{1}{4}$. Moreover, we visualize the differences between f -divergences normalized with respect to $f''(1)$ and χ^2 divergence, for $\epsilon \in [0, 0.01]$. We can see in Fig. 8b, all the differences are very small. This verifies that all f -divergences such that $f''(1) > 0$ satisfy $\frac{2}{f''(1)}D_f(P, Q) = \chi^2(P, Q)$ up to $\mathcal{O}(\epsilon^3)$.



(a) Common f -divergences between such P and Q for $\epsilon \in [0, 0.5]$. (b) Differences between f -divergences normalized with respect to $f''(1)$ and χ^2 divergence for $\epsilon \in [0, 0.01]$.

Figure 8. Common f -divergences between two-sided ϵ -close distributions P, Q , where Q is the 1-dimensional unit Gaussian and $P(x) = (1 + \epsilon \sin(x)) Q(x)$. In (a), we compare these f -divergences for $\epsilon \in [0, 0.5]$. In (b), we verify the conclusion of Lemma 14: $\frac{2}{f''(1)}D_f(P, Q) = \chi^2(P, Q) + \mathcal{O}(\epsilon^3)$.